1990ApJ...360..448H

THE ASTROPHYSICAL JOURNAL, 360:448–464, 1990 September 10
© 1990. The American Astronomical Society. All rights reserved. Printed in U.S.A.

THE VELOCITY FIELD IN THE LOCAL SUPERCLUSTER

MINGSHENG HAN AND JEREMY MOULD
Division of Physics, Mathematics, and Astronomy, California Institute of Technology
Received 1989 October 6; accepted 1990 March 14

ABSTRACT

The velocity field in the Local Supercluster (LSC) is studied using a spiral galaxy sample out to 3000 km s^{-1}. We describe the field with a model that includes spherically symmetric Virgocentric infall, "great attractor" (GA) infall, and random motion of the "Local Anomaly" with respect to its surroundings. The model is optimized using a maximum-likelihood method, which is able to reduce various sample selection effects. Our best estimates for the amplitudes of the Virgocentric and the GA flow at the position of the Local Group (LG) are, respectively, 197 ± 37 and 400 ± 91 km s^{-1}. The Local Anomaly shows a motion of 230 km s^{-1} toward $(l, b) = (205°, 11°)$ with an effective radius of 540 km s^{-1}. The total peculiar velocity of the LG with respect to the GA agrees very well with its motion in the cosmic microwave background (CMB) frame. Our fitting method is able to compare the mass and galaxy number distributions, and implies that galaxies are more clustered than the underlying mass in the LSC. The Hubble velocity of the Virgo Cluster, as a self-adjusted scale parameter in our model fit, is found to be 1422 ± 43 km s^{-1}, which corresponds to a Hubble constant of $(90 \pm 3) \times 10^{-0.2(\mu-31)}$ km s^{-1}, if μ is the distance modulus of Virgo. Finally, Monte Carlo experiments are performed to test the reliability of our fitting technique. An interesting result from the experiments is that the GA's tidal effect on the LSC cannot be misinterpreted as part of the Virgo flow, when the GA infall is turned off in the model fit. Instead, the LG's total velocity toward Virgo would be underestimated, which in turn would cause us to underestimate the Hubble velocity of the Virgo Cluster. The Monte Carlo experiments are also used to estimate the observed scatter in the Tully-Fisher (TF) relation due to random motions of galaxies in the LSC, which then allows us to estimate the intrinsic dispersion of the TF relation. If the peculiar velocity dispersion of galaxies in the LSC is 200 km s^{-1}, we find an upper limit to the intrinsic dispersion of the TF relation of 0.36 mag.

Subject headings: galaxies: clustering — galaxies: Local Group — galaxies: redshifts

I. INTRODUCTION

The dipole anisotropy in the cosmic microwave background (CMB) has conventionally been interpreted as the result of the motion of the Local Group (LG) at a velocity of about 600 km s^{-1} with respect to the CMB (Fixsen, Cheng, and Wilkinson 1983; Lubin *et al.* 1985). This motion is partly due to the infall velocity of the LG into the Virgo Cluster (Peebles 1976; Tonry and Davis 1981; Kraan-Korteweg 1985); the extra part is most easily understood as a bulk motion of the LSC induced by another mass concentration beyond it. It has been pointed out that the Hydra-Centaurus supercluster in the southern sky might be the source of this bulk motion (Shaya 1984; Tammann and Sandage 1985; Lilje, Yahil, and Jones 1986, hereafter LYJ; Aaronson *et al.* 1986). Recent investigations based on an all-sky elliptical galaxy survey led the "Seven Samurai" (Dressler *et al.* 1987; Lynden-Bell *et al.* 1988, hereafter L7S) to propose a very attractive model in which the Hydra-Centaurus supercluster itself is participating in this bulk flow. The source of this bulk flow, nicknamed the "great attractor," is roughly at 4200 km s^{-1}, some distance behind the Centaurus Cluster; the infall velocity toward the GA at the LG has been previously reported to be 500 km s^{-1}, much larger than that toward the Virgo Cluster.

A large radial velocity survey of the GA region by Dressler (1988) shows two prominent peaks at 3000 and 4500 km s^{-1}. The latter has been preliminarily attributed to the GA. Faber and Burstein (1988, hereafter FB) tested their GA model against two nearby spiral samples by carefully fitting the data to a velocity field model in which both the Virgo and the GA infalls have been taken into account. They found that "the spiral samples agree well in a formal sense with the GA–Virgo model," and that "the Virgocentric infall models are heavily modified by the inclusion of the GA flow" because of the strong tidal effect of the GA.

In order to understand the velocity field of the local universe and its sources, a velocity field model is usually constructed and is fitted to an observational data set. In doing this, one has to estimate the distances to galaxies from a "distance indicator" (e.g., the Tully-Fisher [TF] relation, the Faber-Jackson relation). The basic requirements for such a distance indicator are, first, that it must be *universal* within some required accuracy, and, second, that it must not be biased. Investigations so far, as regards the universality of the TF relation, seem to favor a positive result (Bothun *et al.* 1984; Mould, Han, and Bothun 1989; see, however, Djorgovski, de Carvalho, and Han 1989). Biasing effects in distance indicators have recently been widely studied (see Bottinelli *et al.* 1988 and references therein). The Malmquist effect for a magnitude-limited sample and the related density variation effect are probably the most important biasing factors for the purpose of studying the velocity field of the Local Supercluster. An accurate estimate of these effects depends on the detailed knowledge of the luminosity function and the density distribution of galaxies. The simple assumption of a Gaussian luminosity function and constant density distribution may merely be able to remove the "zero point" of the total bias and leave the systematic component. Imagine a data set sampled from a non-Gaussian luminosity function (LF). When a correction with the assumption of a Gaussian LF is applied, one in fact "unfairly" corrects the bright half and the faint half of the sample galaxies.

© American Astronomical Society • Provided by the NASA Astrophysics Data System

1990ApJ...360..448H

This may lead directly to a biased TF slope. Similarly, when a correction with the assumption of constant density is applied to a sample which, in reality, has a density variation on the sample scale, then the velocity field model parameters will be biased. It is therefore essential to remove all these biasing effects in fitting a velocity field model.

In this paper, we seek to study the LSC velocity field using an almost identical model to that of FB, which includes the two mass concentrations at the GA and Virgo, and assume linear spherical symmetric infall (we call it a *linear bi-infall model*). We conduct a formally complete maximum-likelihood procedure, in which the Malmquist effect and the (large-scale) density variation effect can be suitably removed.

II. THE MAXIMUM-LIKELIHOOD PROCEDURE

a) The Formally Complete Maximum-Likelihood Function

The velocity field model is in the Appendix. Once such a model is specified, the next big question is how to find the "most reliable" model parameters from our limited observational data. The method of maximum likelihood might be used to fit a data set. Unfortunately, we can never get a *complete* data set; that is, a given observational data set is always biased owing to some selection effects which are usually poorly understood. In the case of fitting a velocity field model, the sample bias affects the final results mainly through the distance indicator, on which any velocity field model has to rely. The distance indicator used in our adopted spiral sample is the Tully-Fisher relation, which suffers from the Malmquist bias (Teerikorpi 1984; Bottinelli *et al.* 1986; Giraud 1987; L7S). Aaronson *et al.* (1982*a*, hereafter A82*a*) attempted to avoid the Malmquist bias by minimizing the velocity width residual. This method, as they pointed out, is not completely free of systematic errors (see also the discussion in L7S). L7S and FB have the Malmquist effect corrected individually for each galaxy by assuming a uniform galaxy distribution. This way of dealing with the bias is, however, not quite self-consistent. We try to correct the sample selection effects as well as the related density variation effect by constructing a formally complete maximum-likelihood function.

The velocity field model is to be fitted to a spiral galaxy sample. Each galaxy is associated with three observables, the radial velocity V, the apparent magnitude m, and the 21 cm line width $\log W$, that is, each galaxy corresponds to a point in the three-dimensional space (V, m, $\log W$). The complete maximum-likelihood function we aim to find is thus the probability that the sample galaxies have a given distribution in this space. First, we need to know the probability of observing a single galaxy at (V, m, $\log W$) in a given direction in the sky, namely, $p(V, m, \log W \mid \hat{\mathbf{r}})$. Let $D(\mathbf{r})$ be the galaxy space density at $\mathbf{r}$, and $\phi(M)$ be the luminosity function (assumed to be independent of position). At position $\mathbf{r}$, the model predicted velocity $V_{\rm pred}$ is given by equation (A5), and the true (or the observed) velocity of a galaxy at $\mathbf{r}$ is assumed to be normally distributed about the model prediction with dispersion σ_V; σ_V may include the noise in the velocity field and the measurement errors. We also assume that the velocity width $\log W$ at fixed absolute magnitude M is normally distributed with dispersion $\sigma_{\log W}$, which includes intrinsic scatter in the TF relation and the measurement errors. Then, in a volume element $r^2\,dr\,d\Omega$ at position $\mathbf{r}$, the number of galaxies with (M, V, $\log W$) in intervals (M, $M + dM$), (V, $V + dV$) and ($\log W$, $\log W + d \log W$), respectively, is expected to be

$$N(V, M, \log W \mid \mathbf{r})dV\,dM\,d(\log W)r^2\,dr\,d\Omega \propto \exp\left[-\frac{(V - V_{\rm pred})^2}{2\sigma_V^2}\right] \exp\left[-\frac{(\log W - \langle \log W\rangle_M)^2}{2\sigma_{\log W}^2}\right] \times D(\mathbf{r})\phi(M)dV\,dM\,d(\log W)r^2\,dr\,d\Omega\ , \quad (1)$$

where $\langle \log W\rangle_M$ is the average value of $\log W$ at constant M, which is independent of how the sample is collected (Schechter 1980). Note that the TF relation comes in through this term. The distribution probability $p(V, m, \log W \mid \hat{\mathbf{r}})$ is contributed by $N(V, M, \log W \mid \mathbf{r})$ at all distances, filtered somehow by sample selection. Define a sample completeness function $c(V, m, \log W)$, which is the fraction of galaxies with given (V, m, $\log W$) that are sampled from the complete population. Write M in terms of m and r in the usual way, $M = m - 5 \log r$ (r is in units of Virgo distance, and the relative distance modulus is defined to be zero at the Virgo center). The distribution probability $p(V, m, \log W \mid \hat{\mathbf{r}})$ is then given by the normalized integral of $N(V, M, \log W \mid \mathbf{r})$, weighted by the completeness function $c(V, m, \log W)$, over all distances in the given direction.

$$p(V, m, \log W \mid \hat{\mathbf{r}}) = \frac{1}{C}\int_0^\infty r^2\,dr[N(V, m - 5 \log r, \log W \mid \hat{\mathbf{r}}) \times c(V, m, \log W)]\ , \quad (2)$$

where

$$C = \int_{-\infty}^{+\infty} dV \int_{-\infty}^{+\infty} dm \int_{-\infty}^{+\infty} d(\log W) \times \int_0^\infty r^2\,dr[N(V, m - 5 \log r, \log W \mid \hat{\mathbf{r}})c(V, m, \log W)]$$

is a normalization factor. The giant probability of finding all the sample galaxies at their observed (V, m, $\log W$) is $P = \prod_i p_i(V, m, \log W \mid \hat{\mathbf{r}})$. The likelihood function is then

$$L = \ln P = \sum_i \ln p_i(V, m, \log W \mid \hat{\mathbf{r}})\ . \quad (3)$$

The free parameters could be all those in the velocity field model (see Appendix), i.e., $\gamma_{\rm V}$, $\gamma_{\rm GA}$, $W_{\rm V}$, $W_{\rm GA}$, $\mathbf{R}_{\rm GA}$, W_R, $\mathbf{U}$, and those in the distance indicator, i.e., intercept a and slope b. We shall, however, choose only ($W_{\rm V}$, $W_{\rm GA}$, W_R, a, b) as our model free parameters, and fix the others from independent considerations (see § IIc). The likelihood L is expected, from a physical point of view, to maximize at a special point in the parameter space; that point is believed to correspond to the most likely model. The formal errors of the model parameters can be estimated from the covariance matrix $[L'']^{-1}$, where L'' is the Hessian matrix at the point. Searching for this particular point in the parameter space is the subject of the next section. Before we do that, however, we have to make the likelihood L a function of the free parameters only.

b) Realization of the Maximum-Likelihood Function

The likelihood function in equation (3) includes three functions which are still unknown. They are the galaxy space density $D(\mathbf{r})$, the luminosity function $\phi(M)$ and the completeness function $c(V, m, \log W)$. The likelihood function L depends on the selection of the galaxy sample through $c(V, m, \log W)$. In this study, we use the spiral galaxy sample of Aaronson *et al.* (1982*b*, hereafter A82*b*). Based on their description of

© American Astronomical Society • Provided by the NASA Astrophysics Data System

1990ApJ...360..448H

the sample selection, the completeness function can be crudely quantified as

$$c(V, m, \log W) = \begin{cases} \left[\exp\left(\frac{m - m_l}{\Delta m}\right) + 1\right]^{-1}, & V \le 3000, \\ 0, & V > 3000. \end{cases} \quad (4)$$

That is, within the sample limit of 3000 km s^{-1}, the completeness of the apparent H-band magnitudes is approximated with the analytical form of Sandage, Tammann, and Yahil (1979), and the velocity width is complete with respect to magnitude. The two extra parameters (m_l, Δm) introduced into the completeness function will be estimated below. For our purpose of fitting a velocity field model, the sample redshift cutoff and the completeness of the sample in the (m, log W)-plane are assumed to be the dominant biasing factors. Equation (4) is just a crude approximation of these restrictions, where we assume a sharp redshift cutoff and ignore the log W selection effect. This is equivalent to assuming that at a given distance within the sample limit, we miss galaxies only because they are too faint. This should be a reasonable assumption because velocity width is somehow correlated with apparent magnitude. It should be pointed out that our understanding about the sample selection is actually very limited, especially concerning the velocity width. Equation (4) might be the most suitable working form of the *real* sample completeness that, currently, we are able to propose. This form of the sample completeness function should allow us to remove most of the selection biases, such as the familiar Malmquist effect. Another possible sample restriction which is not included in equation (4) is the fact that the sample does not have galaxies in the Galactic plane for $|b| < 10°$. This restriction, however, will not bias our model fit, because the likelihood (eq. [3]) is based on the conditional probability $p(V, m, \log W \mid \hat{r})$, i.e., the probability of observing a galaxy at (V, m, log W) in a *given* direction. The nonuniformity of the Galactic extinction across the sky may bias the likelihood by its differential influence on the predicted probabilities $p(V, m, \log W \mid \hat{r})$. This effect could be easily taken into account, since the (relative) variation of the Galactic extinction with position across the hemisphere is fairly well known (see, e.g., Burstein and Heiles 1978). However, we do not think this is necessary in our case, both because the Galactic extinction is reasonably uniform beyond the Galactic plane (as just mentioned, our sample does not have galaxies in the Galactic plane) and because the extinction at the H band is relatively small (about one-tenth of that in the B band). It should also be pointed out that the Virgo triple-valued region does not affect our analysis at all, because we do not predict distances using the distance-velocity relation, i.e., equation (A5). Finally, it must be noticed that other sample restrictions (e.g., the inclination restriction $i > 45°$), which are not correlated with the involved three observables, are not important here, because only the shape of the completeness function, or the relative completeness, is relevant for our purpose. This can be easily seen from equation (2), where any additional terms in the completeness function that are not coupled with V, m, and log W would be canceled out.

We assume that the H-band luminosity function $\phi(M)$ is of the Schechter form

$$\phi(M) \propto x^{\beta} e^{-x}, \quad (5)$$

where $x = \text{dex}\,[-0.4(M - M_*)]$. Since the H-band luminosity function has not been extensively studied so far, no estimates for M_* and β are available in the literature. We estimate these two parameters and the parameters introduced in the completeness function (m_l, Δm) using the statistical procedure of Sandage, Tammann, and Yahil (1979). Dynamical distances given by A82*b* are used to calculate absolute magnitudes. The results are tabulated in Table 1, where the "F sample" denotes the whole data set of A82*b*, while the "G sample" is a subset of the "F sample" (see § III for details).

TABLE 1

LUMINOSITY FUNCTION AND COMPLETENESS FUNCTION

	Luminosity Function		Completeness Function	
Sample	M_*	β	m_l	Δm
G.....	7.36	−0.057	10.70	0.38
F.....	7.47	−0.046	11.62	0.46

NOTE.—M_* is the H-magnitude of an L_* galaxy at Virgo.

Now we consider the last unspecified function in the likelihood, the galaxy number density $D(\mathbf{r})$. In principle, $D(\mathbf{r})$ could be estimated directly from observations, such as from the *IRAS* data (Yahil 1988; Strauss and Davis 1988). In this paper, however, we shall estimate it in a different manner. In the Appendix, we have assumed a power-law *mass* overdensity profile for the LSC and the GA in constructing the velocity field model. Galaxies contribute at least a certain part (if not all) of the total mass. Some sort of relation between the galaxy number density and the underlying mass density is therefore expected. We assume a simple form for this relation: *number density excess* ~ (*mass density excess*)$^{\alpha}$, or

$$D(\mathbf{r}) = \text{const} \times \left[1 + \left(r_V^{-\gamma_V} + \frac{W_{GA}}{W_V} r_{GA}^{-\gamma_{GA}}\right)^{\alpha}\right], \quad (6)$$

where (r_V, W_V) are the galaxy's distance to Virgo and the amplitude of Virgocentric flow at the LG, respectively, and (r_{GA}, W_{GA}) are the galaxy's distance to the GA and the GA infall velocity at the LG, respectively. The index α will be a useful control parameter: $\alpha = 0$ if galaxies are uniformly distributed; $\alpha = 1$ if galaxies trace mass. Because we are dealing with spiral galaxies only, and it is clear that spirals are less clustered than elliptical galaxies (Dressler 1980; Postman and Geller 1984), when $\alpha = 1$, spirals trace mass, elliptical galaxies would be more clustered than mass.

Our adopted density function above is in some sense consistent with the velocity field model. It would be interesting to check how α influences the model fit. Note that the smaller scale clumpiness in the galaxy distribution is not taken into account in the above approximation. As discussed in the Appendix, ignoring smaller scale inhomogeneities is unlikely to produce systematic errors in the final result; however, if we neglect the large-scale variation of the galaxy distribution, we will most probably get a biased result. Previous works known to the authors have all assumed a constant density in correcting the Malmquist effect.

c) *Choice of Free Parameters*

After we specified the completeness function, $c(V, m, \log W)$, the luminosity function, $\phi(M)$, and the galaxy number density, $D(\mathbf{r})$, the likelihood (eq. [3]) is now a known function of the

© American Astronomical Society • Provided by the NASA Astrophysics Data System

1990ApJ...360..448H

following 13 parameters (see Appendix): γ_V, γ_{GA}, W_V, W_{GA}, $\boldsymbol{R}_{GA}$, W_R, $\boldsymbol{U}$, a, and b. It is not, however, appropriate to fit all these parameters, because (1) the likelihood may not be a well-behaved function with so many variables, in the sense that its maximum solution may not be satisfactorily stable; (2) the galaxy sample we employed is redshift-limited within 3000 km s^{-1}; this limitation makes it insensitive to the position of the GA, which lies outside the sample (see FB); (3) FB claimed that the peculiar velocity of the LG is shared by galaxies around it out to some 700 km s^{-1} (see also Brown and Peebles 1987; Sandage 1986); this implies that our assumed peculiar velocity of the LG with respect to its surroundings, $\boldsymbol{U}$, is no longer a simple constant vector but is a varying vector with at least one more variable, which determines the size of the coherent motion; (4) it is possible to evaluate γ_V, γ_{GA}, $\boldsymbol{R}_{GA}$, and $\boldsymbol{U}$ reasonably well from independent considerations. Therefore, we choose only (W_V, W_{GA}, W_R, a, b) as the model free parameters, and fix the others.

i) γ_V *and* γ_{GA}

The mass overdensity distribution in the LSC is usually assumed to be a power law. The exponent of the profile is, however, hardly determined from direct observation; this is primarily because we observed galaxies rather than mass, and also because we are inside the LSC, making it difficult to study the LSC's mass distribution dynamically. Hoffman, Olsen, and Salpeter (1980) studied the mass distribution in the Virgo Cluster by examining the velocity dispersion as a function of radius, and found that the Virgo density falls off with r^{-2} to r^{-3}. This study was, however, limited to the Virgo Cluster, which is roughly the core of the LSC. Yahil, Sandage, and Tammann (1980) have extensively studied the galaxy distribution in the LSC. They found that the galaxy overdensity profile could be approximated by $\sim r^{-2}$. Hoffman and Shaham (1985) gave a theoretical interpretation for the origin of r^{-2} profiles. Thus, a natural and reasonable choice for the LSC mass excess profile would be r^{-2}, which has been widely used in the literature. We shall also assume this form of mass excess profile in our model, for both the LSC and the GA, i.e., $\gamma_V = \gamma_{GA} = 2$. It is noted that our choice for the value of γ_{GA} is very close to that deduced by Aaronson *et al.* (1989, hereafter A89) and FB, who have allowed the parameter to vary in their models.

ii) $\boldsymbol{R}_{GA}$

As mentioned above, our sample, because of its volume limitation, is not ideal for locating the position of the GA, which is supposed to lie far beyond it. So we need to fix the GA's position, $\boldsymbol{R}_{GA}$, in our velocity field model. Where, then, is the GA? The best estimates for the redshift and Galactic coordinates of the GA by FB, based on their elliptical sample, are $V_{GA} = 4200$ km s^{-1}, $l = 309°$, $b = 18°$. A redshift survey (Dressler 1988) in this direction shows two significant concentrations of galaxies at 3000 and 4500 km s^{-1}, respectively,[1] which provides some observational evidence for the GA. In this paper, we assume that the infall center of the GA is at the position derived by FB. The GA's distance R_{GA} used in our velocity field model is the true distance in units of the Virgo distance rather than the observed velocity. The relation between V_{GA} and R_{GA} is given by equation (A9).

iii) $\boldsymbol{U}$*—the Local Anomaly*

In this subsection, we seek to evaluate $\boldsymbol{U}$, the peculiar velocity of the LG with respect to its surroundings or, more precisely, the background flow field. FB have shown that galaxies around the LG out to about 700 km s^{-1} share the peculiar motion of the LG; their estimate for this coherent motion is 360 km s^{-1} toward $b = 199°$, $l = 0°$. They call this region the "Local Anomaly" (LA), and interpret its large peculiar motion as due to the negative gravity of the "Local Void" (Tully and Fisher 1987) in the opposite direction. We note, however, that it is not as straightforward as it seems to deduce $\boldsymbol{U}$ from their evaluation of the size and motion of the LA. This is because the radius of the LA as given by FB was not well defined. By this we mean that we do not know how much the LA, which obviously has no sharp edge, has blended itself with its surroundings at their quoted radius of 700 km s^{-1}. In this paper we reevaluate the properties of the LA by defining an effective radius of the LA, and employing a different method of model fitting, which is presumably less affected by biasing effects.

First of all, we imagine that the LA is such an elastic patch embedded in the LSC. Its center, assumed to be at the LG, has a peculiar velocity of $\boldsymbol{U}_0$ with respect to the background systematic velocity field. The peculiar velocity at the outer part of the patch gradually drops with increasing radius. This simplified picture can be quantified by approximating the peculiar velocity field inside the patch with a convenient form, $\boldsymbol{U}_0/\{1 + \exp[(V - V_{LA})/\sigma_{LA}]\}$, where the variable V is used to locate the position of a galaxy in the patch. We specify V as the observed velocity of a galaxy. V_{LA} is the effective radius of the patch at which the peculiar velocity drops to $\frac{1}{2}\boldsymbol{U}_0$, and σ_{LA} is a parameter that controls the smoothness of blending the patch with its surroundings. We assume a value of 150 km s^{-1} for σ_{LA}, which is the typical three-dimensional rms velocity dispersion in the vicinity of the LG (FB). The peculiar velocity of the LG *with respect to a galaxy at* V can then be approximated by

$$\boldsymbol{U}(V) = \frac{\boldsymbol{U}_0}{1 + e^{-(V - V_{LA})/\sigma_{LA}}} \quad (7)$$

Here the LA is modeled by four parameters, $\boldsymbol{U}_0$ and V_{LA}. A self-consistent way to determine these parameters is to set them as free parameters in the likelihood function (eq. [3]), and then to maximize the likelihood over the parameter space. However, as we have explained above, this will greatly complicate the likelihood function. We therefore try to evaluate these four parameters independently. We note that equation (7) is actually the residual velocity of a galaxy that would be observed, if the background systematic velocity components were removed. In the local region around the LG, a pure Hubble flow might be a good approximation for the background velocity field. If a galaxy at position $\boldsymbol{r}$ has observed velocity V, then one can write

$$H_0 r = V + \boldsymbol{U} \cdot \hat{\boldsymbol{r}} + \epsilon \,, \quad (8)$$

where ϵ is the sum of the contributions from all other velocity sources, which includes both the random component in the velocity field and some systematic terms due to, e.g., the two

[1] Recently, Scaramella *et al.* (1989) analyzed the new *Catalogue of Rich Clusters of Galaxies* of Abell, Corwin, and Olowin (1989). Surprisingly, they found, besides an expected concentration at 4000 km s^{-1}, another strong concentration of clusters of galaxies in almost the same direction, but with the much greater distance of 14,000 km s^{-1}! They claimed that the dynamical influences of these two mass concentrations at the LG were comparable. In the first approximation, the influence of these two mass concentrations, because of their closeness on the hemisphere, make the local samples of galaxies feel they are being pulled by a single attractor—the "great attractor." So the single attractor model (or the GA model) should be a fairly good approximation in studying the velocity field of the local universe.

© American Astronomical Society • Provided by the NASA Astrophysics Data System

1990ApJ...360..448H

mass concentrations at Virgo and the GA. The LA parameters could be obtained by minimizing the velocity residuals (i.e., ϵ) for a sample of nearby galaxies. This method has been widely used in studying the relative motion of the LG with respect to nearby galaxy samples (see, e.g., Peebles 1988; de Vaucouleurs and Peters 1984). FB also used basically the same method in demonstrating the existence of the LA, and in estimating its motion and size. This method, however, probably leads to a biased result because (1) the velocity residual ϵ is not a good random variable, because of the large-scale background systematic velocity field, and (2) the distances to each of the sample galaxies, which have to be specifically determined from distance indicators in order to calculate the velocity residual, are usually biased as a result of sample selection effects. A straightforward approach to suppress the Malmquist bias is to correct it individually for each galaxy in the sample, as FB did. This is of course not a complete correction, as they have noted. A similar correction could be performed to reduce the effect of background systematic velocity field. For example, in our case, the background velocity field is just the bi-infall pattern. We could take an iterative route to derive both the LA parameters and the bi-infall pattern parameters. In this paper, however, we do not adopt this method; instead we intend to use a relatively simple and cheap method which, we think, is also able to reduce the aforementioned biases to some extent.

The method we employed is also a χ^2 minimization procedure, but we minimize the distance ratio residuals rather than the velocity residuals. From equation (8) and the Tully-Fisher relation, $r = 10^{0.2(m-a-b\log W)}$, the distance ratio of galaxies i and j can be written as

$$10^{0.2(\Delta m - b\Delta \log W)} = \frac{V_i + \boldsymbol{U}\cdot\hat{\boldsymbol{r}}_i}{V_j + \boldsymbol{U}\cdot\hat{\boldsymbol{r}}_j} + \eta_{ij}\,. \tag{9}$$

Where the zero point of the Tully-Fisher relation is canceled, this means that the Malmquist effect is largely removed. The parameter η_{ij} is the difference between the true (or the Tully-Fisher relation–predicted) distance ratio and the Local Anomaly model–predicted distance ratio for galaxies i and j. To first order, $\eta_{ij} \sim \epsilon_i/V_j - \epsilon_j V_i/V_j^2$. The value of η is much less coupled than ϵ with the background velocity field, because ϵ is essentially the background velocity field superposed on a random field, while η is a variable that combines the background velocity information at *two* arbitrary field points and blends them with the random velocity sources at the two points. The LA parameters are thus obtained by minimizing the quantity

$$\chi^2 = \sum_{i\neq j} \frac{\eta_{ij}^2}{\sigma_{ij}^2}\,, \tag{10}$$

where η_{ij} is calculated from equation (9). The parameter σ_{ij}, the error in η_{ij}, is estimated from the dispersions both in the Tully-Fisher relation and in the line-of-sight velocity about the model using the standard error propagation formula. We adopt a dispersion in the TF relation of 0.3 mag, and an rms dispersion in line-of-sight velocity of 100 km s^{-1}, respectively. These are typical values for a nearby galaxy sample. The slope of the TF relation is not adjusted in the fit; rather it is fixed at -10. A simple test shows that variation of the slope within a reasonable range has only a weak effect on our results.

The LA solutions are thus carried out on the A82*b* field galaxies inside successively larger spheres centered at the LG. The largest sphere has a radius of 1200 km s^{-1}, which already touches the Virgo Cluster. Galaxies within 6° of Virgo are excluded in our fit. The results are listed in Table 2. Note that both U_0 and V_{LA} show a good trend of convergence when the sample size exceeds 1000 km s^{-1}, which is a good deal greater than the convergent value of V_{LA}, as would be expected. We adopt the average of the last three solutions as our estimate for the LA model; this yields $V_{LA} = 540$ km s^{-1} and $U_0 = 236$ km s^{-1} toward $(l, b) = (205°, 11°)$, as given in the last row in Table 2. Comparing our predicted motion of the LA with that of FB shows an excellent agreement in direction, as should be the case if the LA's motion is indeed caused by the Local Void in the opposite direction. Their favored amplitude of the motion is, however, about 130 km s^{-1} larger than ours. The effective radius of the LA we have derived is not directly comparable to their cited radius of 700 km s^{-1}, which has no clear definition. We also note that our estimated motion of the LA is in good agreement with the LG's peculiar velocity in A82*a* (their solution [3.1]), which is 177 km s^{-1} toward $(l, b) = (214°, 23°)$.

TABLE 2

THE LOCAL ANOMALY

Sample Limit (km s^{-1})	U_0 (km s^{-1})	l	b	V_{LA} (km s^{-1})	N_{gal}
<700	138 ± 39	249° ± 10°	−19° ± 6°	290 ± 121	46
<800	103 ± 25	256 ± 7	8 ± 6	230 ± 99	58
<900	186 ± 48	196 ± 11	22 ± 5	652 ± 72	63
<1000	173 ± 26	201 ± 5	0 ± 3	480 ± 63	76
<1100	287 ± 24	204 ± 4	12 ± 3	583 ± 30	88
<1200	251 ± 18	209 ± 4	17 ± 2	556 ± 26	100
Estimate[a]	236 ± 23	205 ± 4	11 ± 3	540 ± 40	...

[a] This is the average of the last three solutions in the table, which we adopt as our Local Anomaly model.

Of course, it is of interest to ask, is there a physical basis for the Local Anomaly, or is it just a kinematic convenience? A detailed answer to this question lies beyond the scope of this paper, and is more properly addressed to those constructing self-consistent models of the local gravitational field (Yahil 1988; Strauss 1989). However, we have carried out numerical simulations of the effects of the Local Void (Tully and Fisher 1987) on the local velocity field. We lie on the edge of the Local Void. It extends between $b = -60°$ and $b = 60°$ and between $l = 0°$ and $l = 90°$ out to a redshift of 1500–2000 km s^{-1}. We find that if $\gamma_V = 2$ and the mean overdensity of the LSC interior to the LG, δ, is equal to the 2, the Local Void, assuming zero mass inside, adds ~100% to the local acceleration toward Virgo, and its influence region extends to about halfway between the LG and the Virgo center. Interestingly, our estimates above for the velocity amplitude and the effective size of the LA both coincide very well with the simulation result of this toy model. This suggests that a physical basis for the Local Anomaly may exist within the gravitational picture of peculiar velocities, and a detailed gravitational model of the LSC would be a very worthwhile direction to explore.

Returning to the topic of the current paper, we see that, with the results in §§ II*c*(i)–II*c*(iii), the likelihood L (eq. [3]) becomes a known function of our selected model free parameters only. This leads us to the next section, where we search for the most reliable models under various conditions.

III. FITTING THE MODEL

As already mentioned, we use the 308 galaxy sample of A82*b* in our study. This sample contains some 200 galaxies which

© American Astronomical Society • Provided by the NASA Astrophysics Data System

1990ApJ...360..448H

have both diameters and magnitudes given in the *Second Reference Catalogue* (de Vaucouleurs, de Vaucouleurs, and Corwin 1976). FB have shown that this subset ("good data," as they named it) is of higher quality than the full data set. In the following, we use letter "G" to denote this subsample and the letter "F" for the full sample. We will fit the velocity field model using both samples, but with more emphasis on the G sample.

There are still some input parameters in the likelihood function not yet specified. These are the observed velocity of the Virgo Cluster, V_0, the rms dispersion in line-of-sight velocity, σ_V, and the dispersion in the Tully-Fisher relation denoted as $\sigma_{\log W}$. We adopt a value of 1073 km s^{-1} for V_0 (Huchra 1985); this is corrected for the motion of the Galaxy with respect to the LG centroid. Values for σ_V and $\sigma_{\log W}$ are estimated to be 200 km s^{-1} and 0.03, respectively. Variation of the two σ's does not have a significant effect on the model parameters.

a) Results with χ^2 Method

First of all, we apply the conventional χ^2 minimization method (minimizing velocity residuals) to the two data sets to fit different velocity field models. The χ^2 minimization scheme has been widely used in the literature in studying the velocity field of the local universe. It should be recalled that this method completely ignores the distributions of m and log W, which may introduce bias into the fitting result; it is also unable to handle either the redshift cutoff (or incompleteness) of a given data set or the spatial distribution of galaxies along the line of sight, both of which are expected to bias the fit somehow. It is possible to reduce some of the biasing effects mechanically to some extent, by, e.g., multiplying a suitable constant by the estimated distance of each galaxy in the sample, in the hopes of reducing the Malmquist bias. Such corrections are nevertheless incomplete. We do not carry out such corrections in our χ^2 fit. The results from the χ^2 method in this paper are used to compare with the maximum-likelihood (ML) method. They also prove helpful in comparing the goodness of fit of different velocity field models and the qualities of different data sets.

Since the Virgo core of size about 6° is a highly virialized complex, galaxies within this region are not used in our fits. The results of χ^2 fitting for various velocity field models are tabulated in Table 3, where the solution notation, NX, in column (1) means the Nth solution with X sample (X = G or F). The four categories list, respectively, the solutions for four velocity field models (see Appendix for details), namely, the Virgo infall model, which is recovered by setting $W_{GA} = 0$ in equation (A5); the Virgo infall + LSC rotation model; the Virgo–GA infall model and the Virgo–GA infall + LSC rotation model. The LA model of § II is assumed, except for the six decimal numbered solutions, i.e., 1.1G, 1.2G; 3.1G, 3.2G; 5.1G, and 5.2G. For the three ".1" coded solutions, we use FB's LA model, by simply inserting their estimates for the motion and size of the LA into equation (8). For the other three ".2" coded solutions, we assume no LA. The model free parameters are listed in columns (2)–(6): the Virgo infall velocity at the LG, W_V (col. [2]); the GA infall velocity at the LG, W_{GA} (col. [3]); the amplitude of the rotation velocity field at the LG, W_R (col. [4]); and the slope and intercept of the Tully-Fisher relation (cols. [5] and [6]). Column (7) gives the Hubble constant derived from equation (A6), in units of km s^{-1} per Virgo distance. It should be noted that the Hubble constant is not a free parameter in our model, rather, it is completely determined by the velocity field model. Finally, in the last column is the χ^2 value

TABLE 3

MODEL SOLUTIONS WITH χ^2 METHOD

Solution[a] (1)	W_V (2)	W_{GA} (3)	W_R (4)	$-b$ (5)	a (6)	H_0[b] (7)	χ^2/DOF[c] (8)
Virgo Infall Model							
1G.....	201 ± 24	≡0	≡0	10.27 ± 0.21	9.68 ± 0.03	1330 ± 24	0.96
1.1G.....	226 ± 24	≡0	≡0	10.37 ± 0.22	9.65 ± 0.03	1312 ± 24	1.00
1.2G.....	220 ± 24	≡0	≡0	10.37 ± 0.23	9.66 ± 0.03	1302 ± 24	1.04
2F	199 ± 24	≡0	≡0	10.19 ± 0.20	9.64 ± 0.03	1328 ± 24	1.40
Virgo Infall + LSC Rotation Model							
3G.....	202 ± 23	≡0	211 ± 54	10.21 ± 0.21	9.66 ± 0.03	1332 ± 23	0.89
3.1G.....	226 ± 23	≡0	211 ± 55	10.34 ± 0.21	9.64 ± 0.03	1323 ± 23	0.93
3.2G.....	223 ± 23	≡0	202 ± 56	10.33 ± 0.22	9.65 ± 0.03	1304 ± 23	0.98
4F	193 ± 22	≡0	260 ± 52	10.19 ± 0.23	9.65 ± 0.02	1322 ± 22	1.29
Virgo–GA Infall Model							
5G.....	189 ± 23	336 ± 96	≡0	10.03 ± 0.21	9.69 ± 0.03	1399 ± 32	0.92
5.1G.....	214 ± 24	372 ± 99	≡0	10.12 ± 0.22	9.68 ± 0.03	1389 ± 34	0.95
5.2G.....	209 ± 24	358 ± 105	≡0	10.15 ± 0.23	9.68 ± 0.03	1371 ± 35	1.00
6F	180 ± 24	376 ± 98	≡0	10.44 ± 0.21	9.70 ± 0.03	1398 ± 33	1.33
Virgo–GA Infall + LSC Rotation Model							
7G.....	196 ± 23	140 ± 99	178 ± 62	10.10 ± 0.21	9.68 ± 0.03	1360 ± 33	0.89
8G.....	187 ± 24	115 ± 94	216 ± 61	10.50 ± 0.20	9.68 ± 0.03	1344 ± 33	1.28

[a] The letters G or F following each of the solution numbers in col. (1) indicate which sample the model is fitted to. The ".1" coded solutions use the Local Anomaly model of FB, while the ".2" coded solutions simply assume no Local Anomaly. All other solutions apply the Local Anomaly model of § II in this paper.

[b] H_0 is the Hubble constant derived from eq. (A6), in units of km s^{-1} (Virgo distance)$^{-1}$.

[c] DOF = $N - M$, where M is the number of free parameters in the corresponding model, and N is sample size (184 for G sample, 295 for F sample).

© American Astronomical Society • Provided by the NASA Astrophysics Data System

1990ApJ...360..448H

per degree of freedom for each of the solutions, which measures the goodness of fit.

From Table 3, the following conclusions can be drawn immediately:

1. For each of the four velocity models, χ^2 for the G sample is much smaller than for the F sample. This indicates that the G sample is indeed a "good" sample.

2. Comparing, respectively, the solutions 1G, 3G, and 5G with the corresponding solutions 1.2G, 3.2G, and 5.2G, which differ just by having the LA turned off, we see that the velocity field models are improved when the LA is incorporated. This increases the reliability of our LA model, which comes from an independent study. Also, we note that our LA model improves the fit more than FB's does. It is interesting to note that while the LA improves the velocity field models, the model parameters are only mildly affected. The most noticeable change is a decrease in W_V by about 20 km s^{-1}; the LA, however, has a component of 58 km s^{-1} in the Virgo direction.

3. The Virgo infall model is improved by including another velocity component on the LSC scale of either the GA infall or the LSC rotation. On the face of it, the Virgo infall + LSC rotation model fits the data marginally better than the Virgo–GA infall model. In any case, the Virgo infall pattern (W_V) is almost unaffected by either of these two velocity sources. When both of the two velocity sources are turned on, no further improvements are seen in the model fit, and the amplitudes of the two sources at the LG appear to be comparable.

b) *Results with the Maximum-Likelihood Method*

The ML method, as we discussed at length in § II, is practically applied to the data set in this section. Again, galaxies within 6° of Virgo are not used in our fit. Excluding these galaxies should not introduce any bias into our ML fit, because, as we have discussed, an incomplete sky coverage galaxy sample does not bias the likelihood function. Table 4 lists the results of model fit using the ML method, where only the G data set is used. As in Table 3, column (1) of Table 4 lists the assigned identification for each of the solutions, which is of the form NG^{α}, where N is the solution number, "G" means the G sample, and α is the exponent of galaxy number density introduced in § II (see eq. 6). In columns (2)–(6) are the free parameters of the model, i.e., three velocity field parameters (W_V, W_{GA}, and W_R) and two Tully-Fisher parameters (slope and intercept). Columns (7)–(9) list three derived parameters, which are, respectively, the total peculiar velocity of the LG with respect to a reference frame in which the GA is at rest, the component of this peculiar velocity in the direction of the CMB dipole, and the Hubble constant in units of km s^{-1} per Virgo distance. The relative goodness of model fit is estimated by the change of likelihood values, ΔL, given in column (10), which is measured relative to solution $9G^0$, i.e., the solution of the Virgo infall model with the assumption of uniform galaxy spatial distribution.

We fit each velocity model with different α values. The best solution is of course the one that has the largest ΔL value. So solutions $11G^2$, $15G^2$, $19G^2$, and $23G^2$ give us the best estimates for the four velocity field models respectively. Velocity contour diagrams in the supergalactic plane, corresponding to these four best solutions are given in Figures 1*a*–1*d*.

The following conclusions can be drawn from Table 4.

1. All the solutions in Table 4 show that the amplitude of the Virgo infall pattern at the LG is around 200 km s^{-1}, in

TABLE 4

MODEL SOLUTIONS WITH MAXIMUM-LIKELIHOOD METHOD

	FREE PARAMETERS					DERIVED PARAMETERS			
SOLUTION[a] (1)	W_V (2)	W_{GA} (3)	W_R (4)	$-b$ (5)	a (6)	V_{LG} (7)	$V_{LG}\cdot\hat{r}_{CMB}$ (8)	H_0 (9)	ΔL (10)
Virgo Infall Model									
$9G^0$.....	240 ± 36	≡0	≡0	10.91 ± 0.30	9.73 ± 0.04	376 ± 42	269 ± 26	1369 ± 36	≡0
$10G^1$.....	220 ± 24	≡0	≡0	10.88 ± 0.30	9.73 ± 0.05	360 ± 33	256 ± 19	1349 ± 24	40
$11G^2$.....	210 ± 30	≡0	≡0	10.86 ± 0.31	9.73 ± 0.05	352 ± 37	249 ± 23	1339 ± 30	45
$12G^3$.....	205 ± 10	≡0	≡0	10.84 ± 0.37	9.73 ± 0.05	349 ± 46	246 ± 29	1335 ± 40	33
Virgo Infall + LSC Rotation Model									
$13G^0$.....	236 ± 42	≡0	278 ± 88	10.78 ± 0.32	9.70 ± 0.05	394 ± 100	266 ± 49	1365 ± 42	11
$14G^1$.....	214 ± 33	≡0	247 ± 78	10.75 ± 0.30	9.69 ± 0.05	364 ± 87	251 ± 42	1343 ± 33	49
$15G^2$.....	206 ± 37	≡0	242 ± 69	10.73 ± 0.31	9.69 ± 0.05	357 ± 81	246 ± 40	1336 ± 37	54
$16G^3$.....	205 ± 39	≡0	241 ± 77	10.72 ± 0.30	9.70 ± 0.05	356 ± 89	246 ± 44	1334 ± 39	42
Virgo + GA Infall Model									
$17G^0$.....	235 ± 40	406 ± 90	≡0	10.91 ± 0.32	9.78 ± 0.04	612 ± 101	581 ± 76	1464 ± 46	4
$18G^1$.....	209 ± 39	404 ± 94	≡0	10.86 ± 0.31	9.77 ± 0.05	589 ± 104	562 ± 78	1436 ± 45	43
$19G^2$.....	197 ± 37	400 ± 91	≡0	10.87 ± 0.29	9.77 ± 0.05	576 ± 101	551 ± 75	1422 ± 43	56
$20G^2$.....	205 ± 46	496 ± 80	≡0	10.78 ± 0.32	9.66 ± 0.05	664 ± 95	631 ± 70	1370 ± 50	59
$21G^3$.....	193 ± 39	399 ± 102	≡0	10.86 ± 0.33	9.77 ± 0.05	572 ± 112	548 ± 84	1418 ± 46	49
Virgo + GA Infall + LSC Rotation Model									
$22G^1$.....	212 ± 44	221 ± 96	372 ± 96	10.81 ± 0.30	9.73 ± 0.05	635 ± 143	421 ± 90	1396 ± 50	49
$23G^2$.....	206 ± 41	270 ± 98	219 ± 94	10.80 ± 0.33	9.74 ± 0.05	578 ± 145	456 ± 92	1401 ± 48	59
$24G^3$.....	201 ± 40	272 ± 105	246 ± 102	10.77 ± 0.31	9.74 ± 0.05	593 ± 154	451 ± 97	1397 ± 47	53

[a] In the solution notation NG^{α}, N is the solution number, G stands for the G sample, α is the galaxy number density index introduced in § II. Solution 20 assumes that the observed Virgo redshift is 1000 km s^{-1}, instead of 1073 km s^{-1}, which is used for all other solutions. An explanation to each entry in this table is found in the text.

© American Astronomical Society • Provided by the NASA Astrophysics Data System

1990ApJ...360..448H

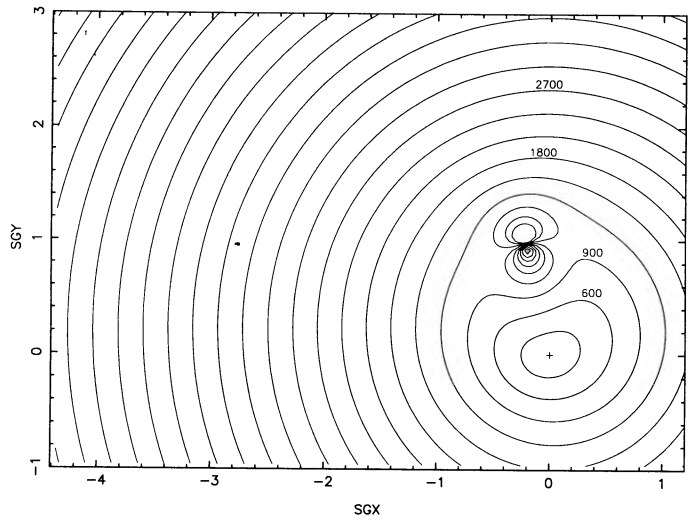

FIG. 1*a*

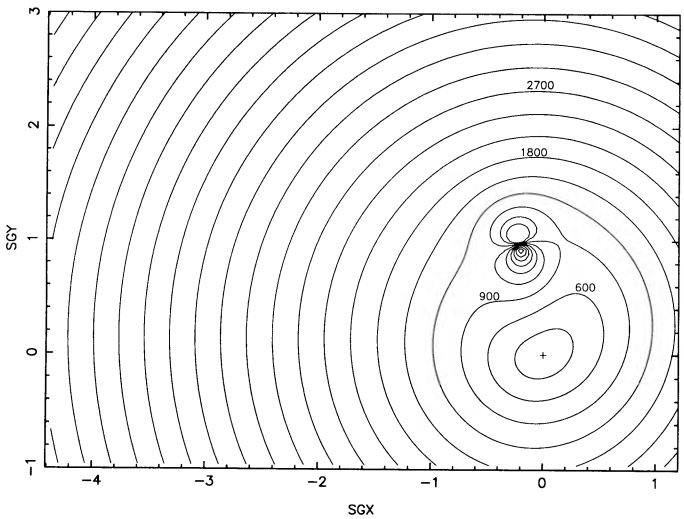

FIG. 1*b*

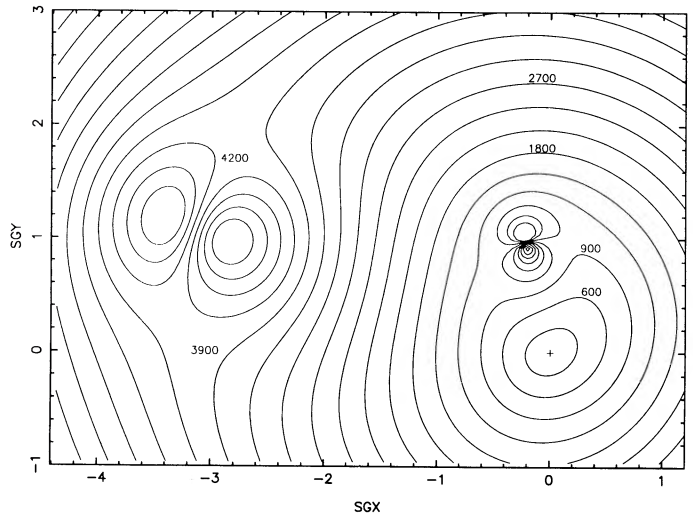

FIG. 1*c*

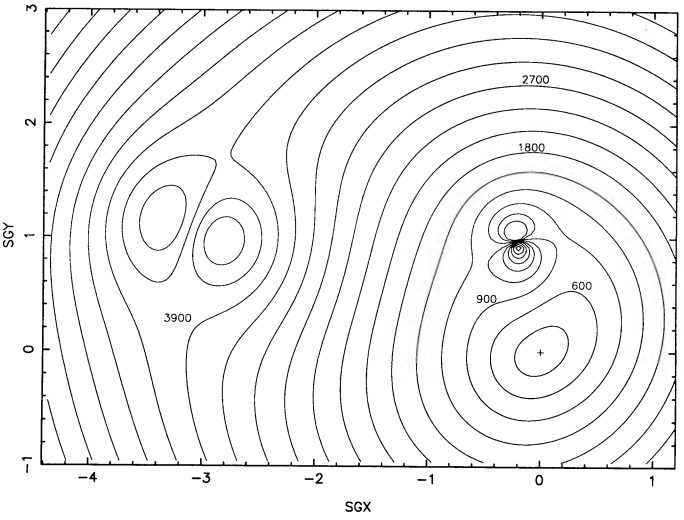

FIG. 1*d*

FIG. 1.—(*a*) Contours of constant observed velocity in the supergalactic plane with contour interval of 300 km s^{-1}. The LG is at the origin; the Virgo Cluster is close to SGX = −0.2, SGY = 1. Distance is in units of distance to Virgo. Model parameters are from solution $11G^2$. (*b*) Contours of constant observed velocity in the supergalactic plane with contour interval of 300 km s^{-1}. The LG is at the origin; the Virgo Cluster is close to SGX = −0.2, SGY = 1. Distance is in units of distance to Virgo. Model parameters are from solution $15G^2$. (*c*) Contours of constant observed velocity in the supergalactic plane with contour interval of 300 km s^{-1}. The LG is at the origin; the Virgo Cluster is close to SGX = −0.2, SGY = 1, and the GA is near SGX = −3.3, SGY = 1. Distance is in units of distance to Virgo. Model parameters are from solution $19G^2$. (*d*) Contours of constant observed velocity in the supergalactic plane with contour interval of 300 km s^{-1}. The LG is at the origin; the Virgo Cluster is close to SGX = −0.2, SGY = 1, and the GA is near SGX = −3.3, SGY = 1. Distance is in units of distance to Virgo. Model parameters are from solution $23G^2$.

good agreement with the conventional value. Our best estimate of the LG infall velocity to the GA is not as large as that of the Seven Samurai.

2. For each of the four velocity field models, the best fit to the data set all occurs at about $\alpha \sim 2$ (more honestly, between 1 and 3). This is clearly seen in Figure 2, where the goodness-of-fit parameter ΔL is plotted against α for all the solutions in Table 4. Recall that the control parameter α is defined such that galaxy traces mass in the form of *galaxy number overdensity* $\propto$ (*mass overdensity*)$^{\alpha}$. So a value of α larger than unity implies that spiral galaxies in the LSC are more clustered than the underlying mass. At the moment we are not able to test the reliability of this statement, but it is interesting to note that all the four velocity field models prefer the same value of α. A numerical simulation in the next section shows that the ML method can detect α reasonably well.

We note that a value of 2 for α roughly corresponds to a r^4 law for spiral galaxy distribution in the LSC, which does not seem to agree well with the empirical r^2 law by Yahil, Sandage, and Tammann (1980). It is not clear whether this is due to merely statistical fluctuations in the two studies or to some other reasons. In any case, the free parameters in our model are not believed to be significantly affected, because, as seen from Table 4, they are very insensitive to the value of α.

3. As can be seen from Figure 2, the Virgo infall model is improved by including either the GA infall or the LSC rotation model or both. Interestingly, the derived amplitude of the Virgo infall field at the LG, W_V, remains the same, regardless of

© American Astronomical Society • Provided by the NASA Astrophysics Data System

1990ApJ...360..448H

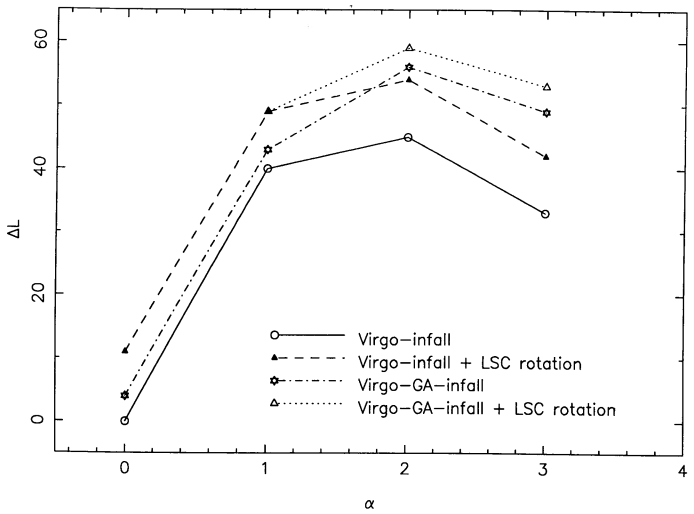

FIG. 2.—Likelihood change ΔL for the ML fitting solutions in Table 4 vs. control parameter α. Different velocity models correspond to different plotting symbols.

which velocity field model is used. It should not be surprising that the LSC rotation has little effect on the Virgo infall, because they are perpendicular to each other. The GA infall, however, produces substantial tidal compression in the LG–Virgo direction, which can influence either the Virgo infall field (see eq. [A3]) or the Hubble constant (eq. [A4]). Our solution shows that the effect of the GA tidal compression is largely to increase the Hubble expansion velocity of Virgo (i.e., to increase the Hubble constant). This is also seen by comparing the velocity contour diagrams (Figs. 1*a* and 1*c*), where the constant velocity contours show little shift against each other in the LG–Virgo direction. Our numerical simulation in the next section also shows that the GA tidal compression does not prevent us from drawing the correct Virgo infall amplitude, even if the GA infall component is not included in the velocity model. Contrary to our conclusion, FB found, while not allowing the Hubble constant to change in their model, that the tidal effect of the GA greatly decreases the Virgo infall amplitude (W_V in our notation). We also fitted our bi-infall model with the Hubble constant fixed at some constant value. We do find that W_V becomes smaller, but not as small as FB found. For example, when H_0 is fixed at 1350 km s^{-1} per Virgo distance, we get $W_V = 164$ km s^{-1} and $W_{GA} = 238$ km s^{-1}.

4. Solution 20G^2 is obtained by assuming a smaller value of $V_0 = 1000$ km s^{-1} for the observed Virgo velocity in the model fit. It is interesting to note that the Virgo infall amplitude is again not affected by change of this model input parameter (see also A82*a*). The derived Hubble velocity of Virgo is consequently reduced, although the increase of the GA infall W_{GA} provides more tidal compression and thus acts to compensate. The intercept of the TF relation is seen to become brighter by about 0.1 mag, which is consistent with the amount of the decrease in the Hubble velocity of Virgo from a simple scaling law. We also note that the likelihood value for this solution is a little higher than that of its corresponding solution 19G^2. We do not know whether this has any implication for the true value of the observed velocity of the Virgo mass concentration. In any case, we learn from this example that using an incorrect observed velocity of Virgo in the model may not bias W_V, but it may significantly affect W_{GA} and the Hubble constant.

5. The total peculiar velocity of the LG with respect to the GA (col. [7]) as predicted by the Virgo–GA infall model agrees fairly well with the LG motion in the CMB frame, both in direction and in magnitude, as can be seen by comparing the value in column (7) with that in column (8), and with the 3 K dipole anisotropy 600 km s^{-1}. Thus, the motion of the LG with respect to the CMB appears to be explained completely by three peculiar velocity sources, namely, the Virgocentric infall at $\sim$200 km s^{-1}, the GA infall at $\sim$400 km s^{-1} and the Local Anomaly at $\sim$240 km s^{-1} toward $(l, b) \sim (205°, 11°)$. This is one reason we prefer the Virgo–GA infall model; solution 19G^2 gives the best estimate of this model.

6. Although the Virgo infall + LSC rotation model and the bi-infall + LSC rotation model are both as good as the bi-infall model according to ΔL, neither is able to reproduce the CMB dipole motion.

It is interesting to ask how the velocity field solution is affected by the input parameter σ_V, the velocity dispersion about the model. We have carried out the Virgo–GA infall solutions for $\sigma_V = 150$ km s^{-1} and $\sigma_V = 250$ km s^{-1}, respectively. These are compared with solution 19G^2 in Table 4, which has used a value of 200 km s^{-1} for σ_V. We found that, relative to solution 19G^2, the likelihood value for the solution with $\sigma_V = 150$ km s^{-1} increased by 2, and that with $\sigma_V = 250$ km s^{-1} decreased by 6. In either case, the model parameters have very little change (well within 1 σ).

Some interesting conclusions can be drawn by comparing the ML fitting results in Table 4 with the χ^2 fitting results in Table 3. First, the two different fitting methods yield the same value for the amplitude of the Virgo infall, W_V, while it is known that the χ^2 method is biased because of Malmquist and other sample selection effects. The implication might be that these biasing factors affect only the scale factor in the velocity model, which, as we have learned from solution 20G^2, does not correlate with the Virgo infall component in the model. Second, the GA infall amplitudes from the two methods are seen to show some differences, indicating the existence of coupling between the GA model and the sample biasing factors. It is therefore important to reduce sample biases in order to obtain the correct GA model parameters. Third, the TF slope from the χ^2 method is slightly shallower than that from the ML method, and the intercept from the χ^2 method is brighter than from the ML method. These differences are in the sense one would expect from the Malmquist bias effect.

In this paper the velocity field has been modeled in the linear approximation. This is a valid approximation in respect of the more distant component due to the GA, which for all galaxies in the present sample represents an overdensity less than unity. But the linear approximation is not a satisfactory approximation in respect of Virgo, especially for galaxies closer to Virgo than we are. Two tests were carried out to estimate the effects of making this approximation on the parameters deduced for the local velocity field. In the first test we generated a counterfeit sample which has the same space distribution as our G sample, and precisely follows a *nonlinear* Virgocentric infall model. To do this, we simply replaced the observed velocity of each galaxy in the G sample by that calculated from equation (6) of Schechter (1980) using the TF distance. We then fitted the linear Virgocentric infall model to minimize the difference between the predicted linear velocities and the nonlinear ones. For a reasonable nonlinear flow model (i.e., the infall velocity at the LG is around 200–300 km s^{-1}), we found that the linear equation underestimated the local infall velocity toward Virgo by $\sim$10%–20%. Note that this conclu-

© American Astronomical Society • Provided by the NASA Astrophysics Data System

1990ApJ...360..448H

sion refers to the G sample with galaxies inside 6° of Virgo excluded. In the second test we deleted the galaxies within 20° of Virgo from the present sample, and found an infall velocity toward Virgo also about 10% more than our best current solution, and little change in the other three model parameters. We conclude that the linear approximation biases our estimate of the local infall velocity toward Virgo to a value which is too low by approximately 20–40 km s^{-1}.

c) *Monte Carlo Experiment*

In order to test the reliability of the ML method, we have performed numerical experiments. A counterfeit data set was generated, which has the same number of galaxies as the real data set (G sample). The coordinate of each simulated galaxy was taken to be that of each real galaxy. The "observed parameters" of each "galaxy" (i.e., apparent magnitude, velocity, and H I line width) were then generated in the following procedure. (1) The distance to each simulated galaxy was generated so that its line-of-sight density distribution in the direction is the same as that of the real galaxy as given by equation (6). (2) The velocity of the galaxy was calculated using a given field model at that distance, and then perturbed by a Gaussian noise with $\sigma_V = 200$ km s^{-1}. (3) The galaxy's luminosity was drawn from a Schechter luminosity function and then filtered by the sample selection function, equation (4). The parameters in the luminosity function and the selection function were taken from Table 1. (4) Finally, the H I line width was derived from the TF relation, with random perturbations drawn from a normal distribution of width $\sigma_{\log W} = 0.03$. A counterfeit data set was thus produced, and the ML fitting method could then be applied to it, exactly as we did to the real data set. In our experiments, two such data sets were produced, using solution 19G[2] in Table 4 as the input models. The average results of fitting a Virgo–GA infall model to these two data sets are listed in Table 5. The first five columns show the input or output model parameters. Column (6) is the control parameter α, which is the index parameter introduced in defining the galaxy number density in equation (6). A model fit on each data set was performed with four different α values, including the input one. The likelihood of each solution (col [7]) was scaled so that the likelihood of the solution with the input α value is zero. Among the four solutions, the best fit, by definition, is the one which has the largest likelihood value. This is the first solution in Table 5. It is seen that the model parameters detected by the ML technique agree quite well with the input parameters within the formal errors. On the other hand, the ML method is also expected to reproduce the control parameter α. Therefore, the best-fitting solution should be the one with α equal to or close to the input α value. The best solution in Table 5 is indeed this one, indicating that the ML method is able to detect α to good accuracy. We may roughly set an estimated error on the parameter α of 0.5, within which it could be detected by the ML method. The real data set, as we see above, has yielded a value of 2 for α, which, according to the estimated uncertainty on α, is well beyond unity. This suggests that galaxies in the LSC are more clustered than the mass.

We also carried out an interesting test by fitting a model to a data set generated by a different model. Line 6 of Table 5 gives the result of fitting a Virgo infall model to the data set generated by the Virgo–GA infall model, and line 7 is the result of fitting a Virgo infall + LSC rotation model to the same data set. Comparing these two solutions with the input model parameters, we draw the following conclusions. (1) The amplitude of the Virgocentric flow at the LG can be correctly revealed, with an *incomplete* velocity field model, or, more specifically, the tidal compression of the GA on the LSC cannot be misinterpreted as Virgo infall. (2) The slope of the TF relation is not affected; the zero point is found to be slightly brighter than the "true" value (at about the 1 σ level). (3) There is an indication that the GA's effect could more or less be interpreted as the rotation of the LSC. (4) The major consequence of missing the GA infall component in the velocity field model is that the Hubble constant would be underestimated by about 6%, which is just about the size of the GA tidal compression in the LG–Virgo direction. This is consistent with a brighter zero point of the TF relation as derived.

IV. SCATTER IN THE TULLY-FISHER RELATION

Given a velocity field model, the distance to each galaxy in a real sample can be calculated, assuming that its observed velocity is exactly at the model prediction. We have thus calculated the distances of the G sample galaxies based on solution 19G[2]. For this exercise only, to avoid the problem of the Virgo triple-valued region, we have simply excluded all the galaxies inside a 20° circle surrounding Virgo. The GA triple-valued region does not bother our calculation too much, because it is beyond the LSC, while the galaxies in our sample are believed all inside the LSC. We therefore just adopt the smallest predicted distance for the galaxies in this region. Using the predicted distances, the TF relation of the G sample was then plotted in Figure 3, where the superposed straight line corresponds to the best estimated TF relation given by 19G[2]; three

TABLE 5

NUMERICAL EXPERIMENT USING MAXIMUM-LIKELIHOOD METHOD

W_V	W_{GA}	W_R	$-$Slope $-b$	Intercept a	α[a]	ΔL[b]	Description
197	400	...	10.87	9.77	2	...	Input (Virgo–GA infall model)
183 ± 31	426 ± 66	...	11.02 ± 0.31	9.77 ± 0.03	2	≡0	Fitting result with $\alpha = 2$ = input value
194 ± 30	375 ± 70	...	11.00 ± 0.30	9.75 ± 0.03	0	−29	Fitting result with $\alpha = 0$
188 ± 29	393 ± 64	...	10.99 ± 0.34	9.75 ± 0.04	1	−3	Fitting result with $\alpha = 1$
182 ± 33	440 ± 74	...	11.04 ± 0.35	9.78 ± 0.04	3	−15	Fitting result with $\alpha = 3$
203 ± 21	≡0	...	10.90 ± 0.36	9.71 ± 0.04	2	−16	[c]
203 ± 40	≡0	123 ± 96	10.84 ± 0.39	9.70 ± 0.04	2	−10	[d]

[a] α is a control parameter in the fitting (see § II for its definition).
[b] The likelihoods are measured relative to the solution, with α being equal to the input value.
[c] Result of fitting Virgo infall model to the counterfeit data set generated with Virgo–GA infall model.
[d] Result of fitting Virgo infall + LSC rotation model to the same counterfeit data set.

© American Astronomical Society • Provided by the NASA Astrophysics Data System

1990ApJ...360..448H

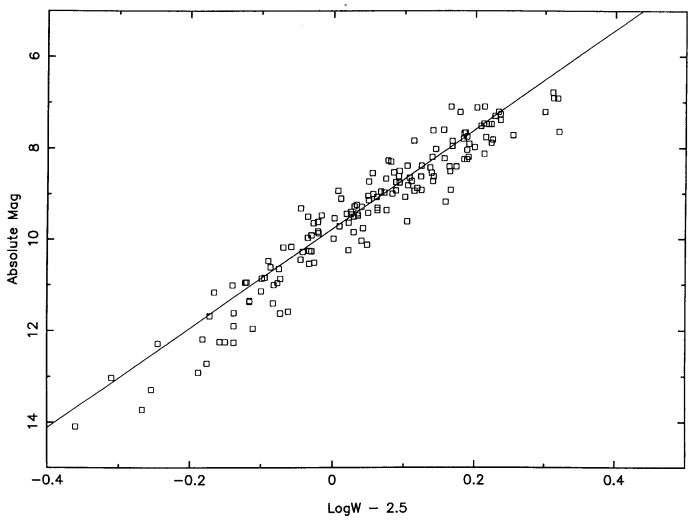

FIG. 3.—Tully-Fisher relation of the G sample. Absolute magnitude is calculated using distance predicted by the Virgo–GA infall model with parameters taken from solution 19G[2]. The superposed line is the best estimated TF relation from the solution.

galaxies with more than 3 σ deviations from this line have been rejected. The scatter about this line was found to be 0.43 mag. This estimate includes, of course, the contribution from the uncertainties in predicted distances, which come from the random motions of galaxies relative to the velocity field model.

A straightforward method to estimate the scatter in the TF relation due to galaxies' random motions is to mimic the situation in Monte Carlo experiments. Assuming a perfect TF relation and the velocity field model as given by solution 19G[2], a counterfeit data set could then be generated following the procedure described in § III*c*. In doing so, one can set the velocity disperision to an arbitrary value to (normally) perturb the simulated velocities. Thus, when we reconstruct the TF relation from such a data set just as we did for the real data set, the scatter in the resultant TF relation would be due purely to the random motions of galaxies relative to the input velocity model. Figures 4*a*–4*d* show four such TF relations corresponding to normal velocity dispersions (σ_V) of, respectively, 150, 200, 250, and 300 km s^{-1}. The mean TF scatter estimates from three experiments for each of these four values of σ_V are listed in Table 6. The "intrinsic" dispersion of the TF relation is estimated to be $[0.43^2 - (\sigma_{TF})^2]^{1/2}$, if σ_{TF} is the simulated TF scatter corresponding to a given velocity dispersion. The last line of Table 6 gives the "intrinsic" dispersion of the TF relation thus calculated, corresponding to each of the assumed random dispersions in the velocity field. Our so-called intrinsic dispersion is actually the scatter of the TF relation that would be observed if there were no random motions of galaxies in the LSC. For example, if the real velocity dispersion in the LSC is 200 km s^{-1}, then the corresponding value of 0.36 mag in Table 6 just sets an upper limit to the true intrinsic dispersion of the TF relation, since it still includes uncertainties due to observations and probably due to a "bad" velocity field model.

V. COMPARISON WITH PREVIOUS WORK

Studies of deviations from pure Hubble flow in the LSC can be roughly categorized into two groups. In the first one, a specific velocity field model is first presumed, such as the infall model with a given number of infall centers. Then the model parameters are adjusted to fit a data set. In the second group the approach is to look for our own motion with respect to some reference frame, which may itself move with respect to the "absolute" frame defined by the CMB (Rubin *et al.* 1976; Aaronson *et al.* 1986). Direct comparison of the results of these two models is difficult. Our study belongs to the first group, and we shall compare our result only with some selected studies from the same group. Even so, it is found that some complications still arise, due to a number of factors. For example, different kinematic models are employed in the studies; different samples with different spatial distribution and different depth and distance indicators are used; different fitting techniques are used; different methods are used to handle the sample selection effects; and even different values for some model input parameters are adopted (e.g., the observed Virgo redshift), or different free parameters are chosen for the same model (e.g., γ is chosen to be a free parameter in some studies but is fixed in others).

In Table 7, we list some selected results for comparison with our own. We choose to compare only the Virgo infall velocity at the LG (W_V), the total peculiar velocity of the LG in the direction of Virgo (W_V^{tot}), and the GA infall velocity at the LG (W_{GA}). Our value for W_V appears to be at the midpoint of those listed in the second column of Table 7. The highest value for W_V in the list is that of LYJ (their solution 3), which is 108 km s^{-1} higher than ours. These authors have used a value for the Virgo redshift of 980 km s^{-1}, which is 93 km s^{-1} lower than the value we adopted. The second highest value of W_V is that of A82*a*, which is 53 km s^{-1} higher than ours. They used a value for the Virgo redshift of 1019 km s^{-1}, which is also lower than the one we used by about 54 km s^{-1}. These comparisons seem to indicate that the differences of W_V in the studies are due to the different values adopted for the observed Virgo redshift. However, as we have shown in § III*c*, reducing the observed Virgo velocity has little effect on W_V (see also A82*a*). The difference between our W_V and that of A82*a* and LYJ is therefore unlikely to be easily explained by the fact that we employed different values for the observed Virgo redshift; it must have to do with the fitting techniques and velocity models. Note that both A82*a* and LYJ employed nonlinear Virgo infall models and χ^2 fitting methods. Our difference with A82*a* and LYJ may be partly explained in terms of the linear approximation we made (see § III*b*, where we estimated that the linear approximation underestimates W_V by about 10%). The next highest

TABLE 6

DISPERSION OF THE TF RELATION

PARAMETER	VELOCITY DISPERSION IN EXPERIMENTS σ_V (km s^{-1})			
	150	200	250	300
Corresponding TF scatter σ_{TF}^V (mag)	0.17	0.24	0.30	0.36
Calculated intrinsic TF scatter σ_{TF} (mag)	0.39	0.36	0.31	0.24

© American Astronomical Society • Provided by the NASA Astrophysics Data System

1990ApJ...360..448H

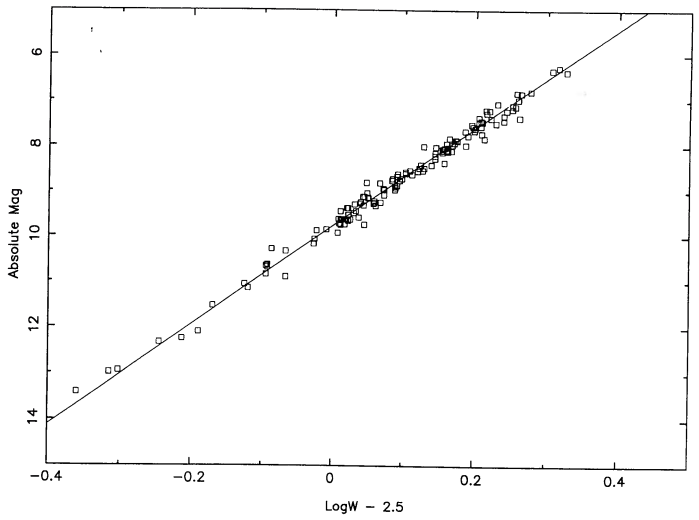

FIG. 4*a*

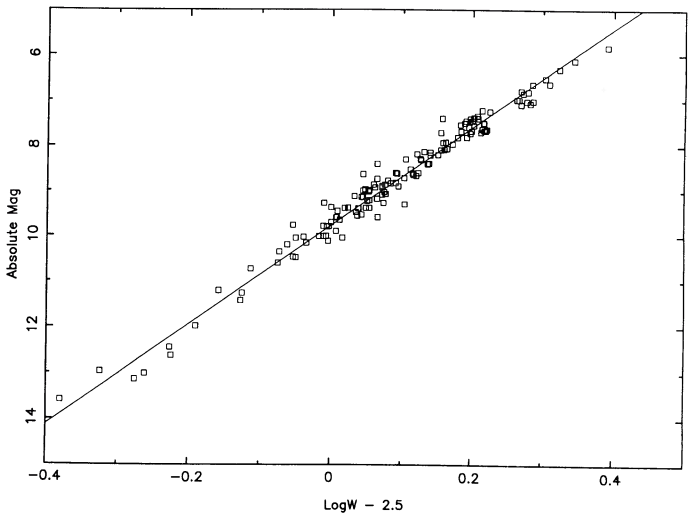

FIG. 4*b*

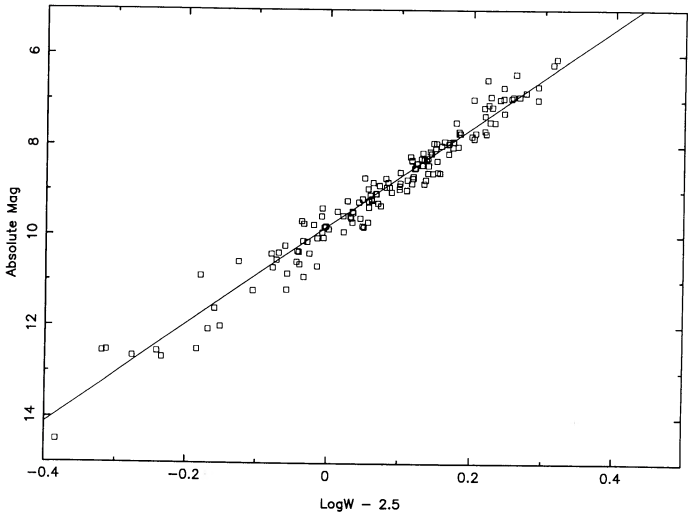

FIG. 4*c*

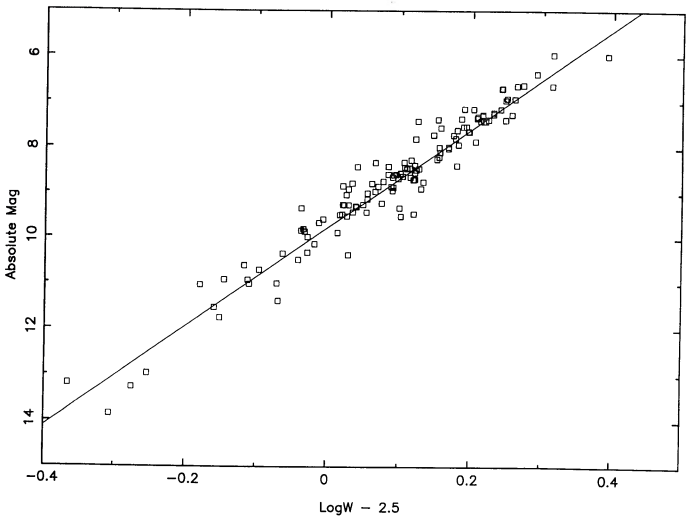

FIG. 4*d*

FIG. 4.—(*a*) Tully-Fisher relation constructed from a counterfeit data set which is generated using a velocity model of solution 19G[2], and assuming a peculiar velocity dispersion relative to the model of 150 km s^{-1}. The scatter seen in the TF relation is completely due to this velocity dispersion. The superposed line is from solution 19G[2]. (*b*) Same as (*a*), but the data set is generated assuming a value of 200 km s^{-1} for the velocity dispersion. (*c*) Same as (*a*), but the data set is generated assuming a value of 250 km s^{-1} for the velocity dispersion. (*d*) Same as (*a*), but the data set is generated assuming a value of 300 km s^{-1} for the velocity dispersion.

value of W_V is that of A89. These authors employed exactly the same kinematic model as we used in this work, the major differences being that they used a χ^2 minimizing scheme to fit a *cluster sample*, and also they did not consider the peculiar velocity of the LG with respect to its surroundings. Our LA model shows that the peculiar velocity of the LG has a component of about 58 km s^{-1} in the Virgo direction. Our difference with A89 is probably mainly due to the missing of this component in their fit. Our estimate of the Virgo infall value is in very good agreement with those of the other listed authors in Table 7, except that of FB and Gudehus (1989). FB found the amplitude of the Virgo infall pattern to be only 85 km s^{-1}. As we mentioned, their prefixed Hubble constant may have some bearing on this low value, because with H_0 fixed, the GA tidal compression in the LG–Virgo direction can only affect the Virgo infall amplitude at LG. However, this is unlikely to be the whole story, as we have tested using our own fitting technique in § III. Since the data set used by FB is the same as we used, the disagreement between our results and theirs may thus lie in the different fitting and sample-bias–reducing techniques employed, or the slight difference in the velocity field models; they have modified the linear infall formula by introducing cores to Virgo and the GA. The other interesting study is that of Gudehus (1989), who obtained a negative amplitude of the Virgo infall pattern of -80 km s^{-1}, using a Hubble diagram technique, which requires a number of careful corrections to the observables.

The third column of Table 7 is the total peculiar velocity of the LG toward the Virgo center, W_V^{tot}. Our result agrees extremely well with those of A82*a*, A89, LYJ, and Staveley-Smith and Davies (1989). The agreement with Peebles (1988) and Tammann and Sandage (1985) is not as good, but these authors used more nearby galaxy samples and did not pay much attention to the possible tidal compression due to an outer mass concentration, or to the peculiar motion of the LG on even smaller scales.

© American Astronomical Society • Provided by the NASA Astrophysics Data System

1990ApJ...360..448H

TABLE 7

COMPARISON WITH OTHER RESULTS

Reference	W_V	W_V^{tot}	W_{GA}	Remark
Present work	197 ± 37	349 ± 43	400 ± 91	Solution 19G[2] in Table 4
A82*a*	250 ± 64	331 ± 41	...	$V_V = 1019$ km s^{-1}
A89	240 ± 37	387 ± 41	486 ± 60	Sample of 20 clusters
Lilje, Yahil, and Jones 1986	315 ± 49	361 ± 85	503 ± 75	[a]
L7S	$\equiv 250$	...	570 ± 60	E galaxy sample
FB	$85 \pm \sim 30$	...	$555 \pm \sim 70$	[b]
Peebles 1988	160 ± 62	160 ± 62	...	Sample range $V < 900$ km s^{-1}
Tammann and Sandage 1985	200 ± 50	200 ± 50	...	Galaxy groups within $800 < V < 1200$ km s^{-1}
Staveley-Smith and Davies 1989	150 ± 60	340 ± 70	543 ± 68	GA in Centaurus Cluster
Gudehus 1989	-80 ± 112	...	...	Hubble diagram technique

[a] A quadrupolar tidal velocity field in the LSC was first detected by these authors, using the same data set as we employed in this paper. Their W_{GA} value listed here does not have exactly the same meaning as ours; see text for details.

[b] FB have fitted a nearly identical velocity field model to the same data set as we used, but using different fitting techniques.

Among the GA infall studies, our agreement with others is generally good, though these results are based on different galaxy samples and on different models or fitting techniques. The position of the GA in the sky derived or adopted by these authors is generally in the same direction, but minor differences exist. In our model, the direction of GA is fixed at that derived by FB, which is about 10° away from that of L7S. Staveley-Smith and Davies (1989) found that the GA lies in the Centaurus Cluster. These authors also considered infalls to other attractors. The observed redshift of the GA is at about 4200 km s^{-1}, as found by FB and adopted in this paper. This, according to equation (A8) and solution 19G[2], corresponds to a true distance of 3.3 in units of the Virgo distance, which is in very good agreement with A89, who also found a value of 3.3.

A quadrupolar tidal velocity field in the LSC was first detected by LYJ. They also used the galaxy sample of A82*b* (the F sample, as we call it in this paper), and found that the eigenvector associated with the largest positive eigenvalue of the quadrupole points in the direction of $(l, b) = (308°, 13°)$, which agrees very well with the GA direction derived by FB and adopted in this paper. With the CMB dipole constraint, they calculated the residual bulk velocity of the LG relative to the CMB of about 500 km s^{-1} in the same general direction; this agrees well with our value of W_{GA}, although two quantities do not have exactly the same meaning. Pretending that this bulk velocity and the tidal velocity field were produced by a single attractor, they estimated the distance of the attractor to be 3 (in units of the Virgo distance), which is also in good agreement with our estimate of the GA distance.

VI. COSMOLOGICAL IMPLICATIONS

a) The Hubble Constant H_0

The Hubble constant is one of the most important parameters in cosmology. In our model, the Hubble velocity of the Virgo Cluster is a self-adjusted scale parameter, and yet it is also an important by-product of our model fit. Our preferred solution yields a value of 1422 ± 43 km s^{-1} for the Hubble velocity of the Virgo Cluster. Let μ be the distance modulus of the Virgo Cluster; we have the Hubble constant $H_0 = (90 \pm 3)10^{-0.2(\mu - 31)}$. Van den Bergh (1989) has recently reviewed the distance scale problem, and has derived a mean Virgo distance modulus $\mu = 31.5 \pm 0.2$, or $d = 20 \pm 2$ Mpc. Adopting this value for the Virgo distance, we get immediately $H_0 = 71 \pm 4$ km s^{-1} Mpc^{-1}. Van den Bergh's quoted uncertainty is very optimistic (see, for example, Burstein and Raychaudhury 1989; Bottinelli, Gouguenheim, and Teerikorpi 1988; Kraan-Korteweg, Cameron, and Tammann 1988; Pierce and Tully 1988; Tully 1989). A reliable value of μ must await extension of the classical distance scale to Virgo with *Hubble Space Telescope* (Aaronson and Mould 1986).

Most of the determinations of H_0 in the literature are based on the Virgo Cluster, and the controversy arises from both the disagreement on the distance to the Virgo Cluster and on the different derived or adopted Hubble velocities of the cluster. Our preferred value for the latter (1422 km s^{-1}) seems to be slightly higher than those derived or adopted in most of previous studies. In our model, the Hubble velocity of the Virgo Cluster is calculated by adding up four separate components, that is, the observed velocity of the Virgo Cluster V_o, for which we adopted a value of 1073 km s^{-1}, the LA component in the Virgo direction of 58 km s^{-1}, the Virgocentric flow of 197 km s^{-1}, and the GA tidal compression of 94 km s^{-1}. This latter component, as we have shown in § III*c*, cannot be "absorbed" by the Virgo infall component, if one just uses a Virgo infall model. The consequence is that the Hubble constant is underestimated, which is indeed what we have noticed in Table 4. The observed velocity of the Virgo cluster, V_o, is an input parameter in our model, on which the Virgocentric flow and the GA tidal compression may somehow depend. That makes the Hubble constant depend on the observed velocity of Virgo in a complicated manner. As was pointed out in § III*b*, when we reduce V_o from 1073 to 1000 km s^{-1} in the model fit, the derived Hubble velocity of Virgo drops from 1422 to 1370 km s^{-1}.

b) The Density Parameter Ω_0

Another interesting parameter in cosmology is the ratio of mean density to the critical density of the universe, the density parameter Ω_0. In the spherical model, the relation between the infall velocity at a distance r from the infall center and the size of a density perturbation δ inside r is well approximated by (Yahil 1985; Regös and Geller 1989)

$$W = \tfrac{1}{3} H_0 r \Omega_0^{0.6} \delta (1 + \delta)^{-0.25} \qquad (11)$$

in both linear and nonlinear zones. This equation has been frequently used to put constraints on Ω_0. In our study, the best estimate of the Virgo–GA infall model is given by solution 19G[2] in Table 4, where the magnitudes of Virgo and GA infall at the LG, are, respectively, $W_V = 197 \pm 37$ km s^{-1} and $W_{GA} = 400 \pm 91$ km s^{-1}, and the Hubble constant $H_0 = 1422 \pm 43$ km s^{-1} per Virgo distance. For the LSC, $r \equiv 1$, and equation (11) gives $\Omega_0^{0.6} \delta (1 + \delta)^{-0.25} = 0.42 \pm 0.08$. Davis *et*

© American Astronomical Society • Provided by the NASA Astrophysics Data System

1990ApJ...360..448H

al. (1980) have estimated the LSC overdensity inside the LG to be $\delta \sim 2$; we thus have $\Omega_0 = 0.12 \pm 0.03$. A similar estimate can be made from the GA infall value. Our distance to the GA in units of Virgo distance is 3.3; we then have $\Omega_0^{0.6}\delta(1+\delta)^{-0.25} = 0.26 \pm 0.06$. Dressler (1988), based on a galaxy survey in the GA region, has roughly estimated the galaxy overdensity within a sphere centered on the position of the GA, of radius reaching to the LG, as $\delta = 1.5$, with an unspecified uncertainty. This yields $\Omega_0 = 0.08 \pm 0.02$, which is in satisfactory agreement with the value obtained from the Virgo infall. It should be noted that the amplitudes of the Virgo and GA overdensities are both derived assuming that galaxies trace the mass. If galaxies are more clustered than mass as proposed by Kaiser (1984), and also as implied by our solution, then the above estimates of Ω_0 can only be regarded as lower limits. To make $\Omega_0 = 1$, as favored by the inflation model, the required biasing factor would be as large as 5, which seems to rule out *standard* cold dark matter (CDM) models with biasing factor $b \sim 2.5$ and $\Omega_0 = 1$ (Kaiser 1988; Bertschinger and Juszkiewicz 1988). We should note, however, that our derivation of Ω_0 may not be reliable because of a number of factors. First of all, equation (11) depends on the assumption of a spherical model, which is obviously not exactly true for both the LSC and the GA structures. Second, fluctuations in the galaxy distribution on various scales are quite common in the local universe (Dressler 1988; Tully and Fisher 1987), and random velocities above the infall pattern induced by irregularities in the local density distribution, such as the LA, may vary greatly from place to place and could be comparable to the amplitude of the underlying infall pattern; these would make the LSC or the GA structure a very complicated kinematic complex (Yahil 1988; Strauss and Davis 1988). We are not yet quite clear as to how our estimate of Ω_0 is affected by these complications. The problem has been discussed more fully by a number of investigators (e.g., Hoffman and Salpeter 1982; Villumsen and Davis 1986).

c) *The LSC Rotation*

In the gravitational instability picture of galaxy formation, a protostructure could be set in rotation by tidal torques from its neighbors. *N*-body simulations have shown (Efstathiou and Jones 1979) that such a mechanism can induce a median value for the dimensionless spin parameter λ (Peebles 1969) of 0.06. For the LSC, it may not be impossible for the GA and the Perseus-Pisces structure in the opposite direction of the sky to set it in rotation, while not producing too large a motion of the whole cluster. It is, however, not possible to convert our result of the LSC rotation into a unique value of λ (Efstathiou and Barnes 1984). It is noted that the LSC must be a very young rotator, if it is indeed rotating at approximately the amplitude we found. This is because one revolution of the LG in the LSC would take about 40 times the age of the universe. The structure of the local universe happens to be such that most of the mass concentrations outside the LSC, especially the GA structure and the P-P structure, lie nearly in the plane of the LSC; this makes it hard to identify the observed peculiar velocities of local galaxies as rotational or infall. We have shown in our Monte Carlo experiments (§ III*c*) that the GA infall pattern can be misinterpreted as LSC rotation. This might be the simplest explanation of the apparent LSC rotation. The authors prefer this interpretation, especially considering the fact that the GA model nicely predicts the CMB dipole motion.

VII. SUMMARY

Our main results in this paper can be summarized as follows:

1. The velocity field of the LSC is modeled as due to three major sources, namely, the Local Anomaly, linear spherical Virgocentric flow, and the GA infall. Rotation of the LSC is also considered as a possible source. The relevant formulae are given in the Appendix.

2. A maximum-likelihood method for fitting a velocity field model to a spiral sample (with the TF distance indicator) is developed. Sample selection effects, such as those due to sample magnitude limitation, space density variation, and redshift cutoff, could in principle be reduced as long as they are known.

3. Our best estimated picture of the LSC velocity field is parameterized as two combined infall patterns induced by the Virgo Cluster and the GA, with flow amplitudes at the position of the LG of $W_V = 197 \pm 37$ km s^{-1} and $W_{GA} = 400 \pm 91$ km s^{-1}. There is then a Local Anomaly smoothly embedded in this bi-infall pattern. The LA, centered at the LG and gradually diminished with an effective radius of 540 km s^{-1}, is moving toward $(l, b) = (205°, 11°)$ with a peak amplitude of 230 km s^{-1}. The CMB dipole motion of the LG is well reproduced in this velocity field.

4. The GA infall pattern can be misinterpreted as LSC rotation.

5. Our ML fit to the LSC sample interestingly indicates that galaxies in the LSC are more clustered than mass.

6. The ML method is tested using Monte Carlo experiments, by which it is also found that the GA tidal effect on the LSC could not be misinterpreted as part of the Virgo infall, and the Hubble velocity would be underestimated if we missed the GA infall in the velocity field model.

7. Distances to sample galaxies are predicted based on our best estimated velocity model. The TF relation accordingly shows an observed scatter of about 0.43 mag. Random motions of galaxies relative to the model with a dispersion of 200 km s^{-1} would contribute 0.24 mag, which would imply that the intrinsic TF dispersion is less than 0.36 mag.

We would like to thank Drs. Dave Burstein, Sandy Faber, George Djorgovski, Reinaldo de Carvalho, Michael Strauss, and Josh Roth for helpful discussions. This work is supported by NSF 87-21705.

APPENDIX

THE LINEAR BI-INFALL MODEL

The model assumes that, in addition to a random noise component, the observed velocity of a galaxy in the LSC is composed of the following terms: (1) free expansion in an uniform Hubble flow $H_0 d$, (2) linear infall toward the Virgo center V_V, (3) linear infall toward the GA V_{GA}, (4) a component U due to the peculiar motion of the LG with respect to its surroundings, and (5) other possible systematic components of unknown origin, S.

© American Astronomical Society • Provided by the NASA Astrophysics Data System

1990ApJ...360..448H

It should be pointed out that our model is basically a relative velocity field model with respect to the frame defined by the GA and the LSC, though the free expansion term may remind one of an absolute background at first sight. It is important to have all the velocity sources on the scale of the galaxy sample included in a velocity model, because an "incomplete" model would most probably give us an incorrect, not just an incomplete, picture of the real world. A familiar example to stress this is the claim of FB that the Virgo infall value at the LG would be overestimated by missing the GA component in the velocity model (though we do not reach the same conclusion on this point). To make the model formally complete, we have to be aware of the possibility of the existence of the fifth term, $\boldsymbol{S}$, above. This component, if it does exist, may more or less bias our understanding of other sources depending on the relevant scale relative to our sample. When the scale of $\boldsymbol{S}$ is much smaller than the sample scale, owing to clumpiness of the sample, for example, or local streaming, or local nonlinearities, its overall influence is more like a random disturbing source; our model will thus most likely be blurred by missing them, rather than be distorted. At the other extreme, when its scale is much larger compared with the sample, it will act as a superstreaming velocity of the whole sample, and this does not affect our relative velocity field model at all. However, when the scale of this unknown-origin velocity component is comparable to the scale of our sample, as in the case of the rotation of the LSC (de Vaucouleurs 1958; A82*a*) or a tidal effect by the Perseus-Pisces supercluster on the side opposite to the GA (Yahil 1988; Strauss and Davis 1988), our current *incomplete* model will draw us a biased picture of the local universe. Nevertheless, our interpretation of the model-fitting results will have to be based on the assumption that we have modeled all the dominant velocity components in the local universe; and other velocity sources are not important. For the purpose of clarity, we now derive the model formula assuming that $\boldsymbol{S} = 0$. We will consider the special case of the LSC rotation as a possible form of $\boldsymbol{S}$.

Let the profiles of density excess be $r^{-\gamma_V}$ and $r^{-\gamma_{GA}}$ for Virgo and the GA, respectively. Then the linear infall velocities into the two mass concentrations can be written as (Peebles 1976)

$$\boldsymbol{V}_V(\boldsymbol{r}_V) = W_V\left(\frac{r_V}{R_V}\right)^{-\gamma_V}\frac{\boldsymbol{r}_V}{R_V}, \tag{A1}$$

$$\boldsymbol{V}_{GA}(\boldsymbol{r}_{GA}) = W_{GA}\left(\frac{r_{GA}}{R_{GA}}\right)^{-\gamma_{GA}}\frac{\boldsymbol{r}_{GA}}{R_{GA}}, \tag{A2}$$

where W_V, $\boldsymbol{r}_V$, and R_V are, respectively, the amplitude of the Virgo infall pattern at the LG, the distance vector from a field galaxy to the Virgo Cluster, and the distance of the LG from the Virgo Cluster. W_{GA}, $\boldsymbol{r}_{GA}$, and R_{GA} are the corresponding quantities with respect to the GA. The predicted line-of-sight velocity V_{pred} of a galaxy at position $\boldsymbol{d}$ (refer to Fig. 5) would be

$$V_{pred} = H_0 d - [\boldsymbol{V}_V(\boldsymbol{R}_V) - \boldsymbol{V}_V(\boldsymbol{r}_V)]\cdot\hat{\boldsymbol{d}} - [\boldsymbol{V}_{GA}(\boldsymbol{R}_{GA}) - \boldsymbol{V}_{GA}(\boldsymbol{r}_{GA})]\cdot\hat{\boldsymbol{d}} - \boldsymbol{U}\cdot\hat{\boldsymbol{d}}, \tag{A3}$$

where the Hubble constant H_0 is given by

$$H_0 = \frac{V_o + \boldsymbol{V}_V(\boldsymbol{R}_V)\cdot\hat{\boldsymbol{R}}_V + \boldsymbol{V}_{GA}(\boldsymbol{R}_{GA})\cdot\hat{\boldsymbol{R}}_{GA} - \boldsymbol{V}_{GA}(\boldsymbol{R}_{GA} - \boldsymbol{R}_V)\cdot\hat{\boldsymbol{R}}_{GA} + \boldsymbol{U}\cdot\boldsymbol{R}_V}{R_V}. \tag{A4}$$

The numerator gives the velocity that would be observed if there were no other velocity sources. The five terms, in order, have the following meanings: (1) the observed velocity of the Virgo Cluster, (2) the infall velocity of the LG into Virgo, (3) the infall velocity of the LG into the GA projected into the Virgo direction, (4) the infall velocity of the Virgo Cluster into the GA projected into the Virgo direction, (5) the peculiar velocity of the LG projected into the Virgo direction. We express all the distances in units of R_V (i.e., set $R_V = 1$), and let θ_V be the angle between the galaxy and the Virgo Cluster, θ_{GA} the angle between the galaxy and the GA, and ϕ the angle between the Virgo Cluster and the GA. Then, after simple manipulations, equations (A3) and (A4) become

$$\begin{aligned} V_{pred} = {} & (V_o + \boldsymbol{U}\cdot\hat{\boldsymbol{R}}_V)d - \boldsymbol{U}\cdot\hat{\boldsymbol{d}} - W_V(\cos\theta_V - d)(1 - r_V^{-\gamma_V}) \\ & - W_{GA}\left(\cos\theta_{GA} - \frac{d}{R_{GA}}\right)\left[1 - \left(\frac{r_{GA}}{R_{GA}}\right)^{-\gamma_{GA}}\right] - W_{GA}\,d\left(\frac{1}{R_{GA}} - \cos\phi\right)\left[1 - \left(\frac{r}{R_{GA}}\right)^{-\gamma_{GA}}\right], \end{aligned} \tag{A5}$$

$$H_0 = V_o + W_V + W_{GA}\cos\phi + W_{GA}\left(\frac{r}{R_{GA}}\right)^{1-\gamma_{GA}}\left(\frac{1 - R_{GA}\cos\phi}{r}\right) + \boldsymbol{U}\cdot\hat{\boldsymbol{R}}_V. \tag{A6}$$

Here r, r_V, and r_{GA} are given by the following obvious relations:

$$\begin{aligned} r^2 &= 1 + R_{GA}^2 - 2R_{GA}\cos\phi, \\ r_V^2 &= 1 + d^2 - 2d\cos\theta_V, \\ r_{GA}^2 &= R_{GA}^2 + d^2 - 2R_{GA}\,d\cos\theta_{GA}. \end{aligned}$$

The quantity d is the estimated distance to the galaxy in units of the Virgo distance. For spiral galaxies we may use the Tully-Fisher relation

$$d = 10^{0.2[m-a-b(\log W - 2.5)]}. \tag{A7}$$

Note that if we turn off the GA infall, i.e., set $W_{GA} = 0$ in equation (A5), then what is left is just the linear infall equation with a single

© American Astronomical Society • Provided by the NASA Astrophysics Data System

1990ApJ...360..448H

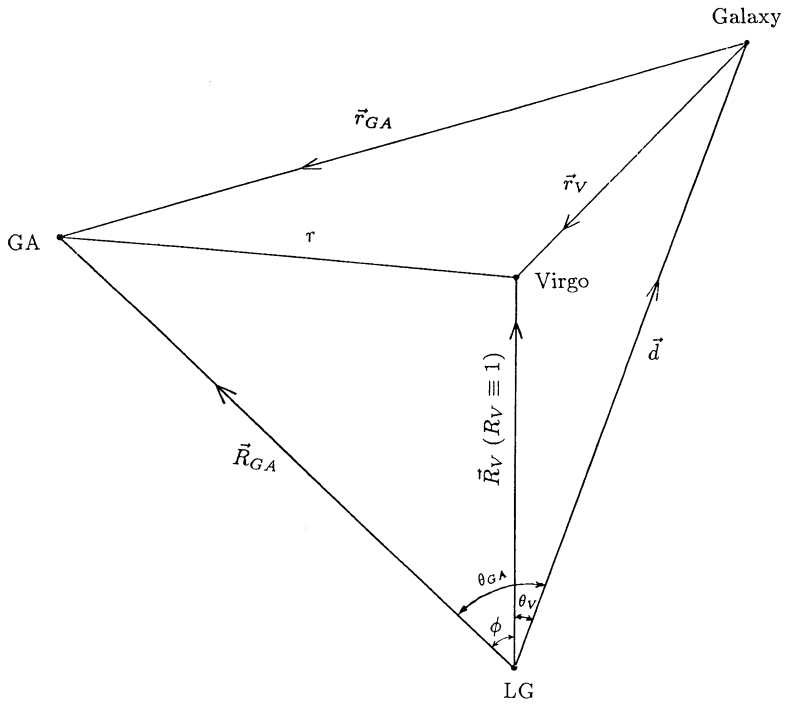

FIG. 5.—Schematic diagram illustrating the geometry referred to in the Appendix

infall center as given by Schechter (1980). Also, it should be noted that the GA distance R_{GA}, in the above equations, is in units of the Virgo distance. The relation between R_{GA} and the observed velocity of the GA, V_{GA}, is given by the following equation:

$$V_{GA} = H_0 R_{GA} - W_{GA} - W_V[\cos\phi + r^{1-\gamma_{GA}}(R_{GA} - \cos\phi)] - \boldsymbol{U}\cdot\hat{\boldsymbol{R}}_{GA}\,, \tag{A8}$$

where all the variables have the same meaning as explained above.

As mentioned earlier, in deriving above formulae, we have set $\boldsymbol{S} = 0$, i.e., assuming no other systematic velocity sources, except the two infall components. We now consider a special case of $\boldsymbol{S}$, the rotation of the Local Supercluster. Following de Vaucouleurs (1958) and A82*a*, we take the rotation field to be of the form $S(r_V) = W_R r_V \exp(1 - r_V^2)$, where W_R is the amplitude of the rotation field at the LG, and r_V is measured in units of our own distance to Virgo. Then the predicted velocity (eq. [A5]) will have an additional component

$$[\boldsymbol{S}(r_V) - \boldsymbol{S}(1)]\cdot\hat{\boldsymbol{d}} = W_R[\exp(1 - r_V^2) - 1]\sin\theta_V\,, \tag{A9}$$

where r_V and θ_V have the same meaning as above. Note that our equation (A9) here is equivalent to equation (8) of A82*a*. Because the rotation velocity field has a zero component in the Virgo direction, the derived Hubble constant (eq. [A6]) remains unchanged.

REFERENCES

Aaronson, M., *et al.* 1989, *Ap. J.*, **338**, 654 (A89).
Aaronson, M., Bothun, G., Mould, J., Huchra, J., Schommer, R., and Cornell, M. 1986, *Ap. J.*, **302**, 536.
Aaronson, M., Huchra, J., Mould, J., Schechter, P. L., and Tully, R. B. 1982*a*, *Ap. J.*, **258**, 64 (A82*a*).
Aaronson, M., *et al.* 1982*b*, *Ap. J. Suppl.*, **50**, 241 (A82*b*).
Aaronson, M., and Mould, J. 1986, *Ap. J.*, **303**, 1.
Abell, G. O., Corwin, H. G., Jr., and Olowin, R. P. 1989, *Ap. J. Suppl.*, **70**, 1.
Bertschinger, E., and Juszkiewicz, R. 1988, *Ap. J.* (*Letters*), **334**, L59.
Bothun, G., *et al.* 1984, *Ap. J.*, **278**, 475.
Bottinelli, L., Gouguenheim, L., Paturel, G., and Teerikorpi, P. 1986, *Astr. Ap.*, **156**, 157.
———. 1988, *Ap. J.*, **328**, 4.
Bottinelli, L., Gouguenheim, L., and Teerikorpi, P. 1988, *Astr. Ap.*, **196**, 17.
Brown, M. E., and Peebles, P. J. E. 1987, *Ap. J.*, **317**, 588.
Burstein, D., and Heiles, C. 1978, *Ap. J.*, **225**, 40.
Burstein, D., and Raychaudhury, S. 1989, *Ap. J.*, **343**, 18.
Davis, M., Tonry, J., Huchra, J., and Latham, D. W. 1989, *Ap. J.* (*Letters*), **238**, L113.
de Vaucouleurs, G. 1958, *A.J.*, **63**, 253.
de Vaucouleurs, G., de Vaucouleurs, A., and Corwin, H. G., Jr. 1976, *Second Reference Catalogue of Bright Galaxies* (Austin: University of Texas,Press).
de Vaucouleurs, G., and Peters, W. L. 1984, *Ap. J.*, **287**, 1.
Djorgovski, G., de Carvalho, R., and Han, M. 1989, in *Extragalactic Distance Scale*, ed. S. van den Bergh and C. Pritchett (San Francisco: ASP), p. 329.
Dressler, A. 1980, *Ap. J.*, **236**, 351.
Dressler, A. 1988, *Ap. J.*, **329**, 519.
Dressler, A., Faber, S., Burstein, D., Davies, R., Lynden-Bell, D., Terlevich, R., and Wegner, G. 1987, *Ap. J.* (*Letters*), **313**, L37.
Efstathiou, G., and Barnes, J. 1984, in *Formation and Evolution of Galaxies and Large Structures in the Universe*, ed. J. Audouze and J. Tran Thanh Van (Gif sur Yvette: Editions Frontières), p. 361.
Efstathiou, G., and Jones, B. J. T. 1979, *M.N.R.A.S.*, **186**, 133.
Faber, S. M., and Burtsein, D. 1988, in *Large Scale Motions in the Universe*, ed. V. C. Rubin and G. Coyne (Princeton: Princeton University Press), p. 115 (FB).
Fixsen, D. J., Cheng, E. S., and Wilkinson, D. T. 1983, *Phys. Rev. Letters*, **50**, 620.
Giraud, E. 1987, *Astr. Ap.*, **174**, 23.
Gudehus, D. H. 1989, *Ap. J.*, **342**, 617.
Hoffman, G., Olsen, D., and Salpeter, E. 1980, *Ap. J.*, **242**, 861.
Hoffman, G., and Salpeter, E. 1982, *Ap. J.*, **263**, 485.
Hoffman, G., and Shaham, J. 1985, *Ap. J.*, **297**, 16.
Huchra, J. 1985, in *Proc. ESO Conf. and Workshop*, No. 20, *The Virgo Cluster*, ed. O. G. Richter and B. Binggeli (Garching: ESO), p. 181.
Kaiser, N. 1984, *Ap. J.* (*Letters*), **284**, L9.
———. 1988, *M.N.R.A.S.*, **231**, 149.
Kraan-Korteweg, R. C. 1985, in *ESO Conf. and Workshop Proc.* No. 20, *The Virgo Cluster*, ed. O. G. Richter and B. Binggeli (Garching: ESO), p. 397.
Kraan-Korteweg, R. C., Cameron, L. M., and Tammann, G. A. 1988, *Ap. J.*, **331**, 620.
Lilje, P. B., Yahil, A., and Jones, B. J. T. 1986, *Ap. J.*, **307**, 91 (LYJ).

© American Astronomical Society • Provided by the NASA Astrophysics Data System

1990ApJ...360..448H

Lubin, P. M., Epstein, G. L., and Smoot, G. F. 1983, *Phys. Rev. Letters*, **50**, 616.
Lubin, P. M., Villela, M. P., Epstein, G. L., and Smoot, G. F. 1985, *Ap. J. (Letters)*, **298**, L1.
Lynden-Bell, D., Faber, S., Burstein, D., Davies, R., Dressler, A., Terlevich, R., and Wegner, G. 1988, *Ap. J.*, **326**, 19 (L7S).
Mould, J., Han, M., and Bothun, G. 1989, *Ap. J.*, **347**, 112.
Peebles, P. J. E. 1969, *Ap. J.*, **155**, 393.
———. 1976, *Ap. J.*, **205**, 318.
———. 1988, *Ap. J.*, **332**, 17.
Pierce, M., and Tully, R. B. 1988, *Ap. J.*, **330**, 579.
Postman, M., and Geller, M. J. 1984, *Ap. J.*, **281**, 95.
Regös, E., and Geller, M. J. 1989, *A.J.*, **98**, 755.
Rubin, V. C., Thonnard, N., Ford, W. K., and Roberts, M. S. 1976, *A.J.*, **81**, 719.
Sandage, A. 1986, *Ap. J.*, **307**, 1.
Sandage, A., Tammann, G. A., and Yahil, A. 1979, *Ap. J.*, **232**, 352.
Scaramella, R., Baiesi-Pillastrini, G., Chincarini, G., Vettolani, G., and Zamorani, G. 1989, *Nature*, **338**, 562.
Schechter, P. L. 1980, *A.J.*, **85**, 801.
Shaya, E. J. 1984, *Ap. J.*, **280**, 470.
Staveley-Smith, L., and Davies, R. D. 1989, *M.N.R.A.S.*, **241**, 787.
Strauss, M. A. 1989, Ph.D. thesis, University of California at Berkeley.
Strauss, M. A., and Davis, M. 1988, in *Large Scale Motions in the Universe*, ed. V. C. Rubin and G. Coyne (Princeton University Press), p. 25.
Tammann, G., and Sandage, A. 1985, *Ap. J.*, **294**, 81.
Teerikorpi, P. 1984, *Astr. Ap.*, **141**, 407.
Tonry, J. M., and Davis, M. 1981, *Ap. J.*, **246**, 680.
Tully, R. B. 1989, *Nature*, **334**, 209.
Tully, R. B., and Fisher, J. R. 1987, *Nearby Galaxies Atlas* (New York: Cambridge University Press).
van den Bergh, S. 1989, *Astr. Ap. Rev.*, **1** (No. 2), 111.
Villumsen, J., and Davis, M. 1986, *Ap. J.*, **308**, 499.
Yahil, A. 1985, in *The Virgo Cluster of Galaxies*, ed. O. G. Richter and B. Binggeli (Garching: ESO), p. 359.
Yahil, A. 1988, in *Large Scale Motions in the Universe*, ed. V. C. Rubin and G. Coyne (Princeton: Princeton University Press), p. 219.
Yahil, A., Sandage, A., and Tammann, G. 1980, *Ap. J.*, **242**, 448.

MINGSHENG HAN and JEREMY MOULD: 105-24 Caltech, Pasadena, CA 91125

© American Astronomical Society • Provided by the NASA Astrophysics Data System